Transportation Research Part E 217 (2027) 105346

Contents lists available at ScienceDirect

Transportation Research Part E

journal homepage: www.elsevier.com/locate/tre

Resilience assessment for China's crude oil shipping network considering maritime chokepoint disruptions☆

Hanwen Fan [a], Lingye Zhang [b], Zhenming Wu [c], Haiying Jia [d,e], Zaili Yang [a,*]

[a] Liverpool Logistics Offshore and Marine Research Institute (LOOM), Liverpool John Moores University, Liverpool, UK
[b] College of Transportation Engineering, Dalian Maritime University, Dalian, China
[c] SNF, Center for Applied Research at Norwegian School of Economics, Bergen, Norway
[d] Department of Business and Management Science, Norwegian School of Economics, Bergen, Norway
[e] Department of Logistics and Maritime Studies, The Hong Kong Polytechnic University, Hung Hom, Hong Kong, China

ARTICLE INFO

Keywords:
Maritime chokepoints
Resilience
Crude oil shipping network
AIS
Maritime transportation
Geopolitical risk

ABSTRACT

Maritime chokepoints face increasing external disruptions from geopolitical conflicts, climate change, and sea accidents, which impose significant risks on global shipping networks and economic prosperity. This study proposes an optimization-based analytical framework to examine the dynamic behavior of network resilience across both disruption and recovery phases. Distinguished from traditional studies that rely on centrality-based indexes to determine critical nodes, the proposed framework identifies worst-case scenario by evaluating specific node failure sequences that induces the maximum resilience performance drop. A dual-optimization framework is then developed to determine the optimal recovery sequence. This framework maximizes the marginal improvement in system performance while explicitly accounting for the node-level recovery priorities. The proposed framework is empirically applied to China's crude oil shipping network, constructed using voyage records derived from AIS that relevant to crude oil tankers serving China's import trade. The analysis identifies a non-linear relationship between resilience loss during the recovery stage and the level of alternative capacity of disrupted maritime chokepoints. Furthermore, the results demonstrate that when critical chokepoints are disrupted, re-routing is not necessarily preferable to targeted recovery efforts. Based on these insights, this study provides a strategic decision-support tool for shipping companies to optimize routing designs and it offers a framework for national governments to safeguard energy security by identifying which chokepoints require prioritized diplomatic cooperation and infrastructure investments.

1. Introduction

Oil and petroleum products remain the dominant energy sources supporting the global economy. However, the geographical mismatch between production and consumption requires long-distance maritime transportation and reliable shipping networks (Si et al., 2026, Sajedianfard and Shahnazi, 2025). Various types of oil tankers serve as the primary carriers, and they transport crude oil

☆ This article is part of a special issue entitled: 'MaritimeSystem_Hans' published in Transportation Research Part E.

* Corresponding author at: Liverpool John Moores University, School of Engineering, Technology and Maritime Operations, Byrom Street, Liverpool, L3 3AF, United Kingdom.
E-mail address: Z.Yang@ljmu.ac.uk (Z. Yang).

https://doi.org/10.1016/j.tre.2026.105346
Received 17 March 2026; Received in revised form 14 October 2026; Accepted 15 October 2026
Available online 2 November 2026
1366-5545/© 2026 The Author(s). Published by Elsevier Ltd. This is an open access article under the CC BY license (http://creativecommons.org/licenses/by/4.0/).

across oceans and through several critical maritime chokepoints to reach their final destinations (Jia and Wu, 2026). In recent years, the stability of these chokepoints has been increasingly threatened by geopolitical conflicts, climate change, and unexpected maritime accidents (Ilyas et al., 2024, Fan et al., 2026b). Consequently, evaluating the resilience of crude oil shipping networks from a systemic perspective has become increasingly important, particularly in understanding network vulnerabilities and how disruptions propagate across interconnected shipping routes.

Although maritime chokepoints are essential to global energy security, they are intrinsically vulnerable because of restricted navigation spaces and the lack of viable alternative routes. Disruptions at these locations have demonstrated their potential to generate severe consequences (Fan et al., 2022, Tran et al., 2024). Recent fluctuations in global oil prices highlight the sensitivity of energy transport to geopolitical tensions, particularly those involving the United States, Israel, and Iran[1,2]. The Strait of Hormuz, a critical maritime chokepoint for global energy transportation, plays a central role in this dynamic. Any potential closure or disruption of this strategic passage would likely cause catastrophic consequences for the global economy. Recently, climate change has also reduced the operational capacity of the Panama Canal, causing significant delays (Fuentes and Munim, 2025). Unlike ports, chokepoints are seen as intermediate nodes that simultaneously affect multiple origin–destination pairs among the ports, thereby triggering rerouting activities and systemic risk propagation across the entire shipping network (Fan et al., 2026a).

Existing studies predominantly conceptualize ports as the primary critical nodes and evaluate system performance under random or targeted port disruptions, particularly within container shipping networks (Liu et al., 2023, Xiao et al., 2024, Wang et al., 2025). While this node-centric perspective captures localized shocks, it is insufficient for maritime chokepoints, where disruptions do not merely remove a link but induce a nonlinear escalation in congestion, transit times, and global transportation costs. The resilience of crude oil shipping networks is further complicated by the heterogeneity of tanker fleets and strict capacity constraints.

In response, recent studies have begun to explore recovery strategies to enhance the resilience of crude oil shipping networks (Su et al., 2025, Su et al., 2026). However, these studies typically adopt a single-objective focused on maximizing connectivity. Such approaches overlook the heterogeneity in recovery priorities of disrupted maritime chokepoints. Ignoring such heterogeneity may lead to idealized recovery strategies that are difficult to implement in real-world emergency management. Recently, a number of studies have begun to explore the resilience of crude oil shipping networks. However, this field remains relatively underdeveloped compared with the extensive body of literature on resilience and safety in other transportation systems. For instance, Shahnazi et al. (2023) used country-level trade data to analyze network shocks. Si et al. (2025) used AIS big data to evaluate the structural resilience of ports from a sub-network perspective. Zhang et al. (2026b) developed a crude oil shipping–trade network and systematically assessed its robustness under realistic disruption scenarios. While these studies provide valuable insights into understanding the crude oil trade patterns and crude oil shipping network resilience performance, a gap remains. The impact of chokepoint failures on network resilience is not yet fully understood, and recovery strategies that balance network performance restoration and recovery priorities of disrupted maritime chokepoints have not been adequately developed. To address this, a chokepoint-failure-oriented resilience assessment framework for the crude oil shipping network is developed in this study. Advanced databases and optimization models are established to simulate both the degradation and recovery phases of the system. This framework provides a reliable tool to analyze cascading disruptions and rational guidance for node recovery decisions.

Given its dominant position in global crude oil imports and heavy reliance on maritime transportation, China is selected as the empirical case in this study (Li et al., 2026). As the world's largest crude oil importer, China relies on a highly diversified maritime shipping network connecting major exporting regions, including the Middle East, Africa, Russia, and South America. These trade flows traverse most of the critical maritime chokepoints, such as the Strait of Hormuz, the Strait of Malacca, the Bab-el-Mandeb Strait, and others. Therefore, China's crude oil shipping network provides a representative and policy-relevant case for examining the resilience performance facing different maritime chokepoint disruption scenarios.

This study aims to holistically analyze the resilience of China's crude oil shipping network under various maritime chokepoint disruption scenarios. From an optimization perspective, recovery strategies are evaluated by considering both network-level resilience restoration and node-level recovery priorities of the disrupted maritime chokepoints. Specifically, the influence of failure sequences on system performance is examined, and rational recovery sequences are identified under uncertainty. To enhance the realism of the simulation, an "alternative routing capability parameter" is introduced to represent the carriers' rerouting behavior. Furthermore, four centrality-based targeted attack strategies are employed as benchmarks to compare the vulnerability assessment results and demonstrate the capability of the proposed framework in identifying worst-case disruption scenarios. The contributions of this study are as follows: (1) A comprehensive crude oil shipping database covering seven vessel types is developed, integrating multi-source datasets to enable high-fidelity network construction. (2) A network resilience assessment method is proposed, explicitly considering maritime chokepoint closures and adaptive rerouting capabilities. (3) New insights into recovery prioritization strategies are provided by balancing network-level resilience restoration and node-level recovery priorities under different alternative routing capabilities.

The remainder of this study is organized as follows. Section 2 reviews the concepts of resilience in maritime systems and define the relevant state-of-the-art for our specific research contributions. Section 3 describes the construction of the crude oil shipping network. Section 4 details the new resilience assessment framework. Following that, Section 5 presents the results of the resilience analysis and provides a comparative analysis. Section 6 summarizes the key findings and discusses the managerial implications for different stakeholders. Finally, Section 7 concludes the study and suggests directions for future research.

[1] https://www.castorvali.com/news/iran-strait-of-hormuz-shipping-crisis-2026/

[2] https://unctad.org/news/hormuz-shipping-disruptions-raise-risks-energy-fertilizers-and-vulnerable-economies

2. Literature review

2.1. Evolution and key concepts of maritime system resilience

The conceptualization of resilience has evolved from a static property of ecological stability into a dynamic systemic attribute within complex engineering and socio-technical systems. Recently, the concept of resilience has shifted toward the systemic ability to anticipate, adapt, and absorb disruptions (Folke et al., 2010). Within the maritime domain, resilience assessment has gained increasing attention. For instance, port resilience is conceptualized as the collective capability of physical infrastructure, operational processes, and institutional governance to withstand and recover from disruptive shocks (Wang et al., 2026, Li et al., 2024, Mohsendokht et al., 2026). Similar concepts have been extended to maritime supply chains and global shipping networks (Yang et al., 2026), highlighting the multi-dimensional nature of resilience in maritime logistics systems (Zhang et al., 2026a, Verschuur et al., 2025, Fan et al., 2026a).

More recently, scholars have introduced the concept of maritime resilience from a dynamic perspective. The shift is largely driven by the inherent complexity of maritime systems, in which the connections between the ports have strengthened and the network structure has become more intricate (Qin et al., 2025). Recent studies underscore that disruptions in such complex systems are rarely localized. Rather, they propagate through spatial-temporal dependencies, triggering cascading failures that compromise overall system performance (Cao et al., 2025b, Zhang et al., 2025b, Zhang et al., 2025a). This complexity necessitates a transition from static topological metrics to dynamic performance assessments. Unlike static structures, the operational efficiency of maritime networks is sensitive to the propagation of delays and the non-linear interactions between maritime and hinterland components (Xin and Yang, 2026). Consequently, traditional static resilience analysis approaches fail to capture the transient behaviors during the external disruptions, necessitating a dynamic perspective.

Based on the prevailing literature, two critical trends in resilience research can be identified. First, there is a shift toward high-fidelity temporal modeling, utilizing time-slice identification to track the system's trajectory from equilibrium through disruption to restoration. Second, the modeling of external shocks has evolved from simplistic, isolated node failures to sophisticated, sequence-dependent disruption scenarios. Despite these advancements, a critical gap remains: current dynamic models often treat recovery as a purely topological restoration, failing to account for the heterogeneous recovery priorities associated with failed maritime chokepoints.

2.2. Review on resilience assessment and optimization on shipping networks

A pivotal shift occurred in the early 2010s when Ducruet and Notteboom (2012) used network centrality-based indicators to identify critical hubs, demonstrating that the global shipping network maintains a degree of robustness despite variations in hub importance. This study marked a transition from traditional statistical approaches to complex network (CN) analysis in maritime studies. Since then, numerous studies have examined the topological properties of regional and global shipping networks using CN-based indicators (Bai et al., 2023, Dong et al., 2020, Shahnazi et al., 2023). For example, Calatayud et al. (2017) utilized six network metrics to assess risk exposure in international freight flows relative to the complex structure of liner shipping networks. Similarly, Poo and Yang (2024) applied centrality analysis to identify the global shipping hubs and the network vulnerabilities. Despite these methodological advances, most existing resilience assessments remain primarily static. As noted by Hu et al. (2026), static indicators are incapable of capturing network evolution during degradation and recovery phases.

Unlike container shipping networks characterized by high connectivity and routing flexibility, the crude oil shipping network exhibits significant spatial rigidity and path dependency. Global crude oil supply chain relies on a few critical maritime chokepoints (Zhang et al., 2026b). The structural concentration makes crude oil shipping networks inherently more vulnerable to chokepoint disruptions than diversified container shipping networks. Consequently, simulation-based stress testing, which is conducted to evaluate system resilience performance under targeted chokepoint failures, cascading disruptions, and flow redistribution scenarios, can reveal the unique failure trajectories of crude oil shipping networks.

With respect to external disruptions, maritime shipping networks are often modeled under isolated, single-event shock scenarios. From a risk management theory perspective, complex infrastructure systems are often evaluated not only under expected conditions but also under extreme or worst-case scenarios to capture systemic vulnerabilities, therefore strengthening the resilience and strategic decision-making. Scenario-based stress testing has been widely used in risk analysis to assess the resilience of interconnected systems when rare but disruptive events occur. Prior studies have investigated the impacts of extreme weather, terrorist attacks, maritime accidents, and global pandemics (Xu et al., 2024b, Gu and Liu, 2025, Verschuur et al., 2023, Shu et al., 2024). Nevertheless, the failure of a single port can trigger cascading effects, leading to congestion or secondary failures throughout the maritime network. These interdependencies are often overlooked in static frameworks but are vital for resilience modeling (Lu et al., 2024).

Recent efforts have introduced node redistribution principles to model cascading failures, incorporating constraints such as regional proximity (Xu et al., 2022), rational service radius (Xu et al., 2024a), and capability constraints (Cao et al., 2025a). While these approaches provide valuable insights into how disruptions propagate from individual node failures, they remain largely focused on isolated events. However, under increasingly volatile global geopolitical conditions, disruptions are increasingly multi-focal and sequential. Traditional cascading models, focusing on isolated triggers, may underestimate the synergistic amplification of system disruptions. Therefore, the resilience boundary of crude oil shipping networks under disruption scenarios, where multiple critical maritime chokepoints fail concurrently, remains poorly understood.

In highly interconnected shipping networks, the disruptions rarely occur as isolated events; instead, they may propagate across the interdependent maritime chokepoints, amplifying their systemic impacts. However, such extreme events typically lie in the tail of the

risk distribution, representing low-probability but high-consequence risks that may generate disproportionate system-wide impacts (Seif et al., 2026, Bei et al., 2019, Wang et al., 2021). In maritime transportation systems, the failure of critical chokepoints can therefore trigger cascading disruptions that propagate through the broader shipping network. Consequently, exploring extreme disruption scenarios through simulation-based analysis can serve as a form of stress testing for the network resilience. Such analysis helps reveal the upper bound of potential systemic losses, providing insights into the failure sequence and resilience degradation trajectory of the crude oil shipping network under cascading disruption mechanisms. These findings are particularly valuable for emergency management and the design of more resilient maritime transport systems.

While identifying the optimal failure sequence clarifies the system's maximum vulnerability, it also dictates the priority and constraints of subsequent recovery efforts. The increasing availability of high-resolution AIS data has further enabled more detailed modeling of maritime network disruptions and recovery processes than traditional trade data and service route data (Chen et al., 2025, Zhu et al., 2025). Recent research has shifted toward developing recovery strategies and optimization-based approaches to bolster network resilience against external disruptions. For example, Wang et al. (2026) utilized shortest recovery time as the primary objective function for post-typhoon restoration modeling. Hu et al. (2026) evaluated resilience through performance ratios, assessing three distinct recovery strategies to optimize system behavior. Su et al. (2026) proposed a framework encompassing increased route capacity redundancy, enhanced node failure tolerance, and optimized recovery sequences to improve the resilience of crude oil shipping networks.

Despite these methodological advancements, existing recovery strategies predominantly prioritize network restoration efficiency, while the heterogeneous recovery priorities associated with different maritime chokepoints remain under-explored. In practical applications, disrupted maritime chokepoints exhibit different levels of strategic importance, recovery urgency, and contributions to the overall resilience restoration of the network. Ignoring such heterogeneity may result in inefficient recovery decisions and prolong the overall restoration process. Therefore, it is essential to simultaneously consider network-level resilience restoration and node-level recovery priorities within the optimization framework to achieve a more balanced and practical recovery strategy for enhancing maritime network resilience.

2.3. Research contributions

(1). A two-stage optimization-based resilience assessment framework under worst-case disruption scenarios is developed.

Unlike existing resilience studies that rely on random failures or centrality-based targeted attacks, the identification of the worst-case failure sequence is formulated as a combinatorial optimization problem, explicitly identifying the disruption sequence that induces the maximum cumulative resilience loss. This optimization-driven degradation analysis enables the identification of the system's resilience boundary and provides a more rigorous stress-testing assessment of network vulnerability. Furthermore, the framework extends the traditional recovery-efficiency-oriented perspective by explicitly balancing the network-level resilience restoration and failed node-level recovery priorities, providing a more realistic representation of recovery strategies decision-making under maritime chokepoint disruption scenarios.

(2). A high-resolution and data-driven model of crude oil shipping networks is constructed.

This study develops a comprehensive, high-resolution crude oil shipping database based on multi-class tanker voyage records derived from AIS data, substantially improving upon traditional trade statistics and static service route data. Collecting voyage-level trajectories of global oil tankers data from Signal Ocean Voyage API, the database covers six tanker categories (e.g., VLCC, Suezmax, Aframax, and others) over a continuous period from January 2022 to December 2023. The proposed data-driven framework reconstructs realistic transportation routes and flow distributions while accounting for vessel heterogeneity and capacity constraints. This integrated modeling approach enables the construction of a dynamic and operationally realistic crude oil shipping network, forming a robust empirical foundation for resilience assessment.

(3). **New insights into recovery prioritization strategies beyond metric-based rules are provided.**

The optimization results demonstrate that nodes traditionally identified as "critical" by static centrality-based indicators are not necessarily optimal targets for failure induction or recovery prioritization. Under different alternative routing capabilities and recovery-priority settings, prioritizing less prominent nodes may yield superior system-level resilience performance. These findings challenge conventional metric-driven decision rules and provide actionable guidance. In practice, the proposed framework also enables the evaluation of potential cargo losses and overall resilience performance of the crude oil shipping network when one or multiple critical maritime chokepoints are disrupted. Such assessments can assist crude oil importing countries in estimating supply risks. From an operational perspective, the results can further support shipping companies in deciding whether to reroute vessels through alternative pathways or temporarily wait for the recovery of disrupted chokepoints, depending on the expected system-level resilience losses and recovery timelines. These insights may serve as an evidence-based foundation for strategic energy security investments, particularly in economies that are highly dependent on crude oil imports.

3. Crude oil shipping network construction

A comprehensive framework for constructing China's crude oil shipping network is presented in this section. The network representation and data handling procedures are outlined in Section 3.1 and 3.2 respectively to ensure methodological rigor and reproducibility.

3.1. Network structure construction theory

The crude oil shipping network serving China's imports is modeled as a weighted directed graph $G(N, E, W)$, where: N is used to denote the set of nodes, including export ports, import ports, and intermediate transit nodes (e.g., straits and canals). E represents the set of directed edges between node pairs, corresponding to crude oil shipping routes. W is used to demote the cargo flows associated with each directed edges, measured by the total crude oil volume transported between node pairs.

To ensure methodological rigor and handle the complexity of maritime big data, Python (Network-X) is applied for network construction. This computational environment provides superior capability in processing multi-attribute edge weights and high efficiency in mapping large-scale trajectory data into a structured topological representation.

In this study, the actual cargo volume is utilized as the primary metric for network flow analysis. The resulting network representation captures both the topological structure and the flow capacity of China's crude oil supply chain.

3.2. Data collection and handling

High-resolution AIS data were collected from the Signal Ocean platform [3], covering the period from January 2022 to December 2023. The dataset includes approximately 9,138 voyages conducted by over 2,406 crude oil tankers, providing detailed spatial-temporal information on vessel movements. A multi-step data cleaning procedure was applied to ensure the quality and reliability of the network, as shown in Fig. 1.

The AIS database contains the necessary information and could be used for tracking and monitoring the ships, and it could also be used for the exchange of the information with other ships (Yang et al., 2019). In addition, the IMO number is used as the unique identifier for each vessel, enabling the integration of AIS trajectories with external vessel information databases. In Step 1, voyages with missing or inconsistent port information, timestamps, or trajectory data were deleted. Following that, in Step 2, IMO identifiers were linked to external databases to retrieve vessel type and capacity. Then, the statistical descriptions of tanker vessels types and number of voyages are summarized in Table 1.

During Step 3, valid transportation routes from loading ports to discharging ports were extracted, and cargo flow were aggregated along each chokepoint. Finally, in Step 4, the final dataset includes node-level information, spatial-temporal voyage details, and cargo characteristics, providing a robust empirical foundation for network construction.

4. Resilience Assessment and Optimization Framework

As shown in Fig. 2, the proposed framework aims to evaluate the crude oil shipping network under maritime chokepoints disruption scenarios by jointly considering the network degradation and recovery processes.

The proposed framework consists of four steps and is highlighted in orange in Fig. 2. Section 4.1 establishes the formal definition and quantitative metrics for China's crude oil shipping network resilience, providing the mathematical basis for performance evaluation. Section 4.2 outlines the fundamental operational assumptions and constraints required for the optimization models.

The rationale behind the framework is that resilience is a dynamic process naturally involving both resilience degradation upon disruptions and resilience restoration process. Therefore, a two-stage optimization structure is adopted to holistically model the worst-case degradation trajectory and the optimal recovery trajectory in Section 4.3. Finally, Section 4.4. illustrates the solution algorithm design.

4.1. Measuring Resilience for China's crude oil shipping network

In this study, the resilience performance of China's crude oil shipping network is defined as the capability of the system to withstand external disruptions, particularly failures occurring at maritime chokepoints. Network resilience performance is quantified using the transportation capacity ratio $Q(t)$ (Su et al., 2025), which represents the proportion of the actual transportation volume relative to the baseline capacity. Fig. 3 presents a conceptual illustration of resilience evolution during the disruption and recovery processes and explains the resilience metric adopted in this study. The temporal evolution of network performance is categorized into four phases, including the initial stable phase, a degradation phase, a recovery phase, and a new equilibrium stable phase. Here, t denotes the discrete time step in the resilience assessment process. During the initial phase, the system remains in a stable operating state, and resilience is subsequently assessed through the dynamic changes occurring throughput the degradation and recovery processes. Finally, the resilience performance reaches a new equilibrium state (Wan et al., 2018).

(1). Normal operation phase (from t_0 to t_1): the crude oil shipping network functions normally, denoted as $Q(t_1)$ during this phase.

(2). Degradation phase (from t_1 to t_2): an external disruption (i.e., maritime chokepoints failures) occurs at time t_1, and then transportation capacity level declines gradually from $Q(t_1)$ to $Q(t_2)$.

(3) Recovery phase (from t_2 to t_3): after time t_2, disrupted maritime chokepoints recover to the pre-disruption level. During this phase, the transportation capacity gradually increases to a new stable state.

(4) New equilibrium state (from t_3 onwards): after the recovery process stabilizes at time t_3, the crude oil shipping network reaches

[3] https://www.thesignalgroup.com/signal-ocean/signal-ocean-platform

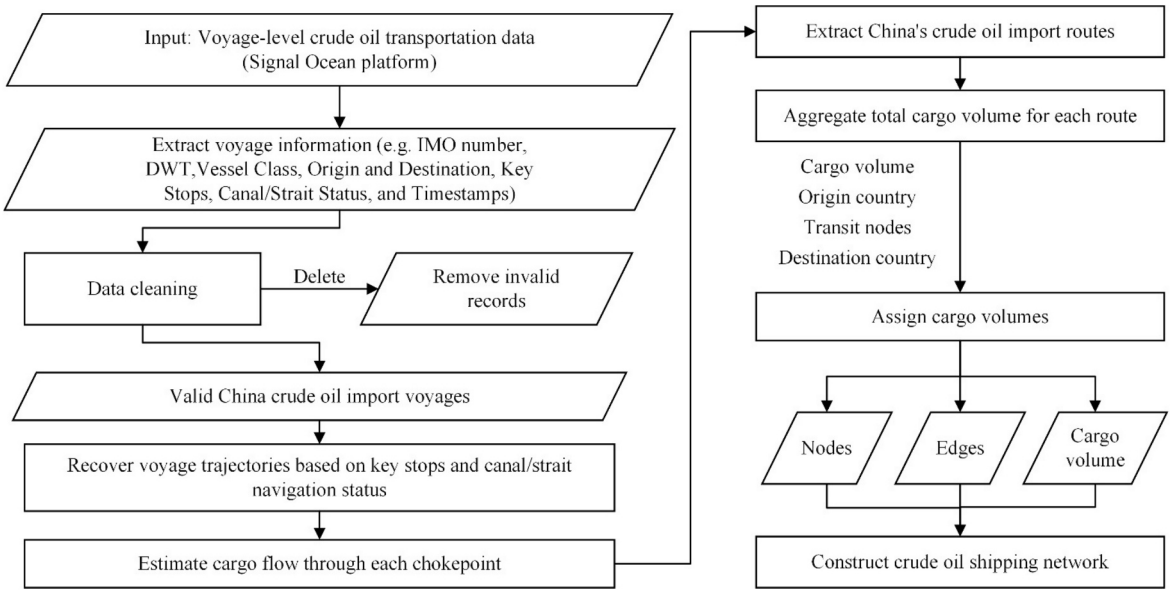

Fig. 1. Data handling process for the crude oil shipping network construction.

Table 1
Descriptive statistics of oil tankers used in this study.

Type	DWT (Unit: tons)	Number of voyages
Very Large Crude oil Carrier	More than180,000+	2825
Suezmax	120,000–179,999	538
Aframax	80,000 – 119,999	1474
Panamax	60,000 – 77,999	239
Medium Range 2	42000—59,999	964
Medium Range 1	32,000 – 41,999	211
Small Tanker	less than 32,000	2887

a new equilibrium state.

Based on the above analysis, the resilience index R of the crude oil shipping network is defined as follows:

$$R = \frac{\int_{t_1}^{t_3} Q(t)dt}{Q(t_1)\times(t_3-t_1)} (1)$$

where, R is bounded with the range of $[0,1]$, and a higher value of R indicates a stronger resilience performance. In the ideal case, when R approaches 1, the network exhibits strong resilience and maintains most of its transportation capability through the disruption and recovery stages.

4.2. Model Assumptions

The following assumptions are utilized for this framework to capture the dynamic resilience change mechanisms of network degradation and recovery phases.

Assumption 1. *Discrete modeling of dynamics and prioritization. The dynamic trajectory of network resilience is modeled as a discrete-time process in which maritime chokepoint nodes fail sequentially according to a predefined disruption rule. At each time step, only one maritime chokepoint is subject to fail, and the corresponding network resilience index is updated. After that, the cumulative impacts of the node failures are used to reflect the dynamic degradation trajectory of the crude oil shipping network.*

Assumption 2:. *Rational stakeholders and constrained optimization. It is assumed that all stakeholders are rational decision-makers. Consequently, they will endeavor to identify optimal alternative routes and make beneficial decisions under finite resource constraints to maximize the system benefits.*

Assumption 3. *Strong correlation between cost and distance. A positive correlation between the route cost and the route distance* (Hu et al., 2026). *This relationship is consistent with typical transportation cost structures.*

Assumption 4. *Absence of infrastructure constraints on alternative routes. It is assumed that the initially selected alternative routes are not subject to infrastructure bottlenecks or capacity constraints.*

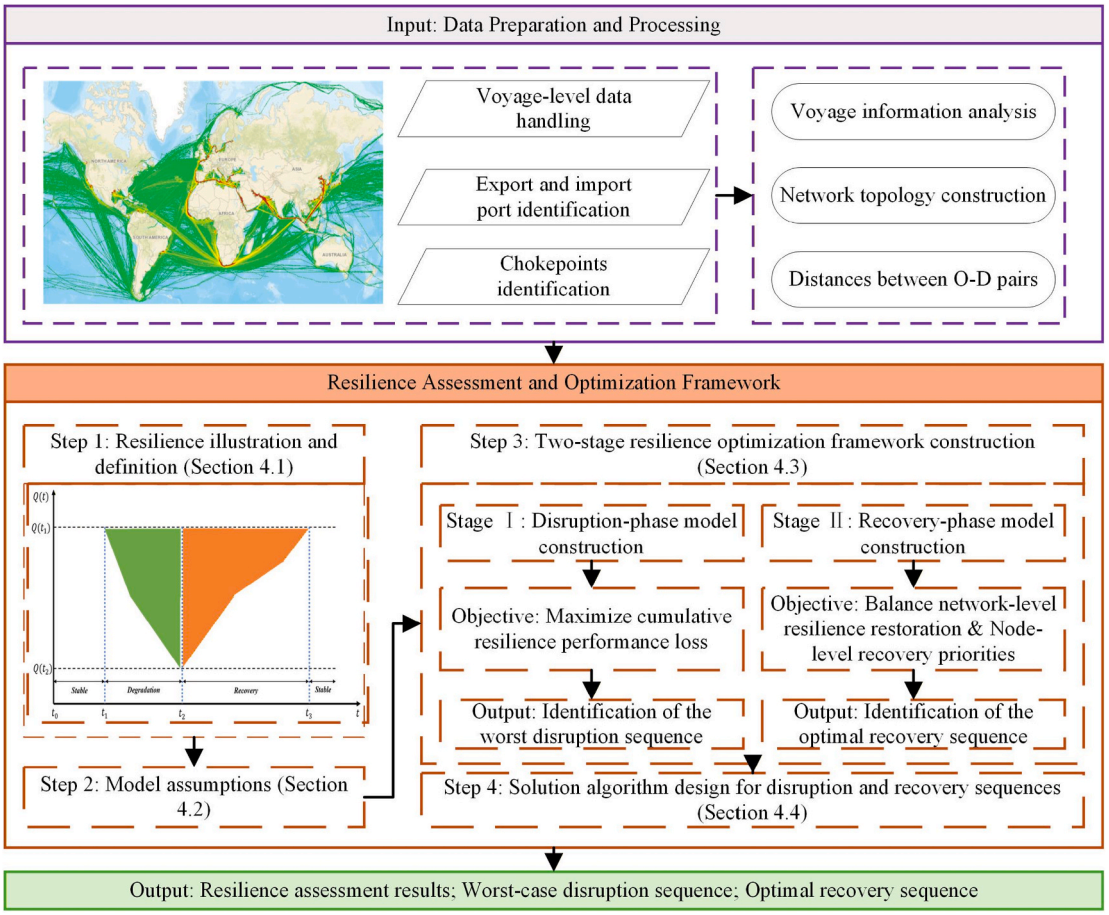

Fig. 2. Resilience assessment and optimization framework process.

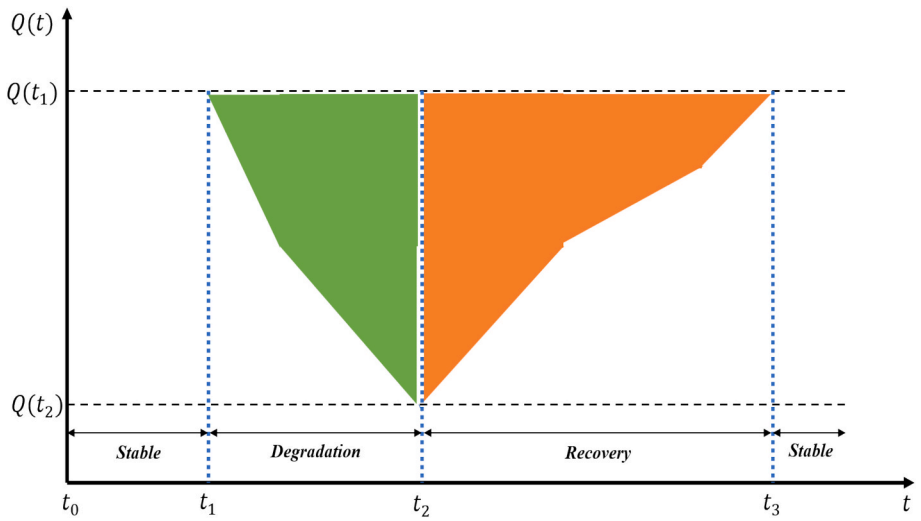

Fig. 3. Theoretical representation of resilience performance.

Assumption 5. *Constrained and prioritized recovery. Restoration resources, including finance, equipment, and personnel, are limited. Consequently, the disrupted maritime chokepoints cannot be restored simultaneously and must follow a sequential order. The recovery sequence is determined by considering the network-level resilience restoration performance along with the recovery priorities of disrupted maritime*

chokepoints.

Assumption 6. *Node failure independence. The failure and recovery of each maritime chokepoint are assumed to be independent of those of other chokepoints.*

4.3. Two-stage resilience optimization framework construction

In this section, a two-stage framework is developed to comprehensively assess the resilience performance of the crude oil shipping network. The proposed framework consists of two sequential and interdependent stages. Stage 1 identifies the worst-case disruption scenario by progressively simulating maritime chokepoint failures and evaluating the resilience loss. Then, the disrupted network state generated in Stage 1 served as the initial network condition for Stage 2, which determines the optimal recovery sequence by balancing network-level resilience restoration performance and node-level recovery priorities of the disrupted maritime chokepoints.

The framework begins with Stage 1: resilience assessment under targeted maritime chokepoints failure scenarios, where network degrades by setting key maritime chokepoints to fail. Following the degradation phase, Stage 2: optimized recovery strategy focuses on determining the optimal restoration sequence. The primary objective of this stage is to balance the overall resilience restoration performance of the maritime network and the heterogeneous recovery priorities of failed maritime chokepoints. This optimization framework yields a best-performing recovery sequence that adheres to specific operational and resource constraints. Ultimately, the output of optimal strategy reveals how the resilience of China's oil shipping network can be restored, allowing the system to gradually return to its normal operational state or evolve toward a new equilibrium under severe disruption conditions. The specific settings, parameters setting, decision parameters setting are summarized in Tables 2–4.

Stage 1: Disrupted phase modelling construction

$$maxZ_1 = \sum_{t \in T_A} (Q_0 - Q(t)) \bullet \Delta t \tag{2}$$

Subject to:

$$Q(t) = \sum_{(i,j) \in W} \sum_{p \in P_{ij}} f_p(t),\ \forall t \in T_A \tag{3}$$

$$\sum_{(i,j) \in W} \sum_{p \in P_{ij}} f_p(t) \le C_E,\ \forall i \in N_E,\ \forall t \in T_A \tag{4}$$

$$\sum_{(i,j) \in W} \sum_{p \in P_{ij}} f_p(t) \le C_I,\ \forall j \in N_I,\ \forall t \in T_A \tag{5}$$

$$\sum_{n \in N_T} x_n(t) - \sum_{n \in N_T} x_n(t-1) = 1,\ \forall t \in T_A \tag{6}$$

$$\sum_{n \in N_T} x_n(t) \le \beta,\ \forall t \in T_A \tag{7}$$

$$|T_A| - 1 = \beta \tag{8}$$

$$x_n(t) - x_n(t-1) \ge 0,\ \forall t \in T_A,\ \forall n \in N_T \tag{9}$$

Table 2
Sets setting and meaning of the proposed framework.

Notation	Meaning
N	The set of all nodes,$N = N_E \cup N_I \cup N_T$
N_E	The set of export nodes
N_I	The set of import nodes
N_T	The set of the transit nodes (including straits and canals)
N_D	The set of disrupted nodes during the recovery phase
W	Set of all origin–destination (OD) pairs, where $w = (i,j), i \in N_E, j \in N_I, w \in W$
P_w	Set of feasible paths connecting OD pairs,$w \in W, p \in P_w$
$P_w(t)$	Set of feasible paths connecting OD pair w at time t, $w \in W$
N_p	Set of nodes included in path p connecting OD pair w, $p \in P_w, N_p \subseteq N$
T_A	Time interval corresponding to the performance degradation phase,$T_A = \{0, 1, 2, \cdots, t_A\}$
T_R	Time interval corresponding to recovery phase,$T_R = \{t_0, t_0+1, \cdots, t_R\}$

Table 3
Parameters setting and meaning of the proposed framework.

Notation	Meaning
L_p	The initial distance of path p connecting the OD pairs,$p \in P_w$
$L_p(t)$	The actual path distance set of path p connecting the OD pairs at time t, $p \in P_w$
$f_p(t)$	The flow volume carried by path p connecting the OD pairs at time t,$p \in P_w$
$F_w(t)$	Total flow volume between the OD pairs at time t, $w \in W$
t_a	Start time of disruption phase, normally $t_a = 0$
t_0	End time of the disruption phase and the start time of the recovery phase.
t_R	the end time of the recovery phase
C_E	Initial target export volume for the exporter nodes at time t_a
C_I	Initial target export volume for the importer nodes at time t_a
F_n	Resilience score of the transit node n, $n \in N_T$
α	Alternative routing capability parameter, if an alternative path exceeds the original path length by a factor of $(1 + \alpha)$, it is unacceptable
β	Maximum number of disrupted maritime chokepoints during the disruption phase.
ε	Resilience recovery priority parameter
Z	Overall resilience restoration optimization objective
Z_1	Network resilience loss objective during the disruption phase
Z_2	Residual resilience loss objective during the recovery phase
Z_3	Recovery-priority objective based on node-level resilience score during the recovery phase

Table 4
Decision parameters setting and meaning of the proposed framework.

Notation	Meaning
$x_n(t)$	One binary parameter, whether the transit node n is disrupted at time t,$n \in N_T$ (1 if disrupted, 0 otherwise)
$\delta_{pq}(t)$	One binary parameter, whether alternative path p is economically feasible compared with the original path q for the same OD pair at time t, (1 if feasible, 0 otherwise)
$z_n(t)$	One binary parameter, whether the disrupted node n is selected for restoration at time t.(1 if restored, 0 otherwise)
$\gamma_{pq(t)}$	One binary parameter, whether path p is selected as shortest economically feasible alternative path for OD pair at time t.(1 if selected, 0 otherwise)

$$\delta_{pq} = \begin{cases} 1, L_p \le (1+\alpha) \bullet L_q \\ 0, otherwise \end{cases}, \forall (i,j) \in W, \forall p, q \in P_{ij} \tag{10}$$

$$L_p(t) = L_p + M \bullet \left(1 - \prod_{n \in N_P} x_n(t)\right), \forall (i,j) \in W, \forall p \in P_{ij}, \forall t \in T_A \tag{11}$$

$$f_p(t) = \begin{cases} F_{ij}(t), if \gamma_{pq(t)} = 1 \\ 0, otherwise \end{cases}, \forall (i,j) \in W, \forall p \in P_{ij}, \forall t \in T_A \tag{12}$$

$$\gamma_{pq(t)} = \begin{cases} 1, if L_p(t) = \min q \in P_{ij} \{ L_q(t) \| L_q(t) < M and \delta_{pq} = 1 \} \\ 0, otherwise \end{cases} \forall (i,j) \in W, \forall t \in T_A, \forall t \in T_A \tag{13}$$

$$x_n(t) \in \{0,1\}, \forall t \in T_A, \forall n \in N_T \tag{14}$$

In Stage 1, the objective function, Equation (2), is employed to maximize the resilience loss when the crude oil shipping network faces external disruptions. This is achieved by strategically simulating discrete node failures, aiming to identify the worst-case disruption scenario. Constraint (3) is used to ensure flow conservation throughout the crude oil shipping network, mandating that the total transport volume flowing into a node equals the volume flowing out across all connected paths at time t.

Constraints (4) and (5) impose boundary volume balance conditions. Specifically, Constraint (4) limits the export volume at each export node i to its predefined maximum level, while Constraint (5) restricts the import volume at each import node j within its planned capacity. Constraints (6) to (9) regulate the number and sequence of disrupted maritime chokepoints. Constraint (6) ensures that at most one additional transit node is disrupted at each time step. Constraint (7) ensures that the cumulative number of disrupted maritime chokepoints does not exceed the predefined maximum. Constraint (8) further guarantees that the total number of simulation periods in the degradation stage is consistent with the number of disrupted nodes. Constraint (9) enforces the monotonically non-increasing nature of the node state, ensuring that nodes, once failed, cannot spontaneously recover within the disrupted phase.

Constraints (10) to (13) regulate the selection of alternative routes within the degraded network. Under the rational decision-maker perspective, the shipping companies are assumed to consider the economically feasible alternative routes when the original routes become unavailable. Constraint (10) acts as a screening mechanism by excluding alternative routes with distances longer than the acceptable threshold defined by the alternative capability parameter . Constraint (11) assigns an extreme penalty to the length of any path containing a failed node, effectively ensuring its exclusion from the feasible solution space during the optimization. Constraint (12) links the path selection decision to the actual flow assignment on the network. Finally, Constraint (13) selects the shortest route among the economically feasible alternatives, ensuring that transportation demand is reassigned through the most feasible alternative

pathway.

The output of the stage 1 serves as the initial input to stage 2. Specifically, the worst-case disruption sequence and the corresponding set of the failed maritime chokepoints identified in Stage 1 define the initial network state for the recovery process. Based on this degraded network configuration, Stage 2 determines the optimal recovery sequence by jointly considering the network-level resilience restoration and the node-level recovery priorities of disrupted maritime chokepoints. Therefore, the resilience restoration optimization problem is directly relied on the disruption outcomes obtained from Stage 1, thereby establishing a sequential and interdependent relationship between network degradation and resilience restoration processes.

Stage 2: Recovery phase modelling construction

$$minZ = \varepsilon Z_2 - (1-\varepsilon)\bullet Z_3 \tag{15}$$

$$minZ_2 = \sum_{t\in T_R}(Q_0 - Q(t)) \bullet \Delta t \tag{16}$$

$$maxZ_3 = \sum_{t\in T_R}\sum_{n\in N_T} z_n(t) \bullet F_n \tag{17}$$

Subject to:

$$Q(t) = \sum_{(i,j)\in W}\sum_{p\in P_{ij}} f_p(t),\ \forall t \in T_R \tag{18}$$

$$L_p(t) = L_p + M \bullet \left(1 - \prod_{n\in N_P} x_n(t)\right),\ \forall (i,j) \in W,\ \forall p \in P_{ij},\ \forall t \in T_R \tag{19}$$

$$\gamma_{pq(t)} = \begin{cases} 1, if L_p(t) = \min q \in P_{ij}\{L_q(t) \| L_q(t) < Mand \delta_{pq} = 1\} \\ 0, otherwise \end{cases} \forall (i,j) \in W,\ \forall t \in T_A, \forall t \in T_R \tag{20}$$

$$\sum_{n\in N_T} z_n(t) - \sum_{n\in N_T} z_n(t-1) = 1,\ \forall t \in T_R \tag{21}$$

$$\sum_{n\in N_T} x_n(t_0) = \sum_{t\in T_R}\sum_{n\in N_T} z_n(t) \tag{22}$$

$$|T_R| - 1 = \beta \tag{23}$$

$$z_n(t) \in \{0,1\},\ \forall t \in T_A,\ \forall n \in N_R \tag{24}$$

Stage 2 focuses on determining the optimal recovery sequence following the network disruption phase. Equation (15) is employed to optimize the node recovery sequence by balancing network-level resilience restoration performance and node-level recovery priorities of disrupted maritime chokepoints. This equation serves as the overall resilience restoration optimization objective. Equation (16) minimizes the residual of resilience loss and Equation (17) maximizes the cumulative resilience contribution of the restored nodes. Constraints (21) to (23) ensure the temporal and logical feasibility of the recovery sequence. Constraint (21) ensures that exactly one disrupted maritime chokepoint is restored at each recovery time step. Constraint (22) ensures the consistency between the number of initially disrupted maritime chokepoints and the cumulative number of recovered maritime chokepoints. Constraint (23) mandates that the total number of time periods utilized in the recovery simulation must precisely equal the total number of maritime chokepoints requiring recovery. All remaining constraints in the recovery model follow the same mathematical formulation as those defined in Stage 1, while operating on the dynamically updated network topology during the resilience restoration process.

4.4. Solution algorithm design

In this section, we present the solution algorithms for both the resilience degradation and recovery stages. The degradation phase employs a recursive exhaustive search procedure, while the restoration phase is formulated as a finite-horizon dynamic programming (DP) problem.

The degradation phase is solved using a recursive exhaustive search procedure that systematically explores all feasible disruption sequences and identifies the worst-case disruption pathway. At each step, one transit node is selected for failure from the remaining candidate set, then then network resilience performance is evaluated. By exhaustively exploring all feasible disruption sequences, the algorithm determines the worst-case disruption pathway that maximizes cumulative resilience loss, thereby revealing the resilience boundary of China's crude oil shipping network.

In contrast, the resilience restoration phase focuses on identifying the optimal recovery sequence by balancing network-level resilience restoration and node-level recovery priorities associated with disrupted maritime chokepoints. The DP model is formally

defined through the following components.

(1) Stage k ($k = 1, 2, \ldots, N_D$): is used to represent the decision point at which the kth node is selected during the recovery phase.

(2) State s: the set of nodes that have already been recovered, where $s \subseteq N_D$.

(3) Decision: at each stage, select one node $n \subseteq N_D \backslash s$ to recover it next step.

(4) Stage return (immediate recovery benefit): $g(s \cup \{n\})$ is used to represent the composite recovery benefit obtained by adding node n to the already-recovered set s.

(5) Value function: $V(s)$ represents the maximum cumulative recovery benefit achievable from the state s onwards, defined as below:

$$V(s) = \max_{\{n \subseteq N_D \backslash s\}} \{g(s \cup \{n\}) + V(s \cup \{n\})\}, \forall s \subseteq N_D, V(N_D) = 0 \tag{25}$$

The optimal total recovery benefit is $Z^* = V(\varnothing)$, and the optimal recovery sequence π^* is reconstructed by tracing the sequence of decisions that achieves $V(\varnothing)$. The pseudocode of the complete algorithm is presented in Table 5.

5. Case study

5.1. Real world crude oil shipping network analysis

China's oil import network is selected for case study to evaluate network resilience with the proposed framework. As the world's largest crude oil importer and the second-largest crude oil consumer, China provides a representative and policy-relevant setting for resilience analysis (Sajedianfard and Shahnazi, 2025). According to the statistic released by the General Administration of Customs of China, the top 10 China's maritime crude oil imports countries are identified and shown in Fig. 4.

The results show that China's primary import routes are highly concentrated on Middle East. Major suppliers in this region include Saudi Arabia, Iraq, the United Arab Emirates, Oman, and Kuwait. Most crude oil from these countries is transported through the Strait of Hormuz and the Strait of Malacca before arriving at its coastal ports. Beyond the Middle East, the network extends to other global regions. Russia remains a key supplier through both Far East and Baltic routes. For Atlantic markets, crude oil from Angola in West Africa typically travels around the Cape of Good Hope, crosses the Indian Ocean, and passes through the Strait of Malacca. Similarly, shipments from South American countries like Brazil and Colombia follow long-distance trans-oceanic routes that also rely on the Strait of Malacca as a final gateway. Additionally, regional trade with Malaysia adds to the shipping density within the South China Sea. These primary routes and corresponding maritime chokepoints are the backbone of China's oil supply, providing the necessary transportation voyages for our resilience analysis in the following sections. Based on the analysis of the real-time global oil tankers shipping network, 16 critical maritime chokepoints are identified and shown in Fig. 5.

Based on the statistical analysis of our shipping database, the probability of each arrival port was calculated as the proportion of voyages arriving at that port relative to the total number of voyages in the dataset. As shown in Fig. 6, Ningbo port, Lanshan port, and Tianjin port are the top three crude oil import ports in China. The connectivity patterns of these ports show their specific geographical roles. Ningbo Port serves as a primary gateway for Middle Eastern oil, with its major routes connecting to Ras Tanura in Saudi Arabia, Basrah in Iraq, Kuwait Port, and Mina Al Fahal in Oman. Because these sources are highly concentrated, most oil shipments for Ningbo must pass through the Strait of Hormuz. Lanshan Port has a more diverse supply, receiving large volumes from Kozmino in Russia alongside Middle Eastern routes from Oman and Saudi Arabia. In contrast, Tianjin Port plays a key role in the Asia-Pacific region. Its main imports come from Ulsan and Yosu in South Korea, Singapore, and Kozmino in Russia. These characteristics show that while

Table 5
Pseudocode of Optimal Recovery Sequence solution algorithm.

Input: N_D: Set of disrupted transit nodes to be recovered, determined at the end of the disruption phase $N_D \subseteq N_T$; F_n: Resilience score of the transit node n, $n \in N_D$; ε: Priority parameter; $g(s)$: Composite recovery benefit obtained by recovering node set s

Output: π^* : Optimal recovery sequence among the failure nodes; Z^*: Maximum cumulative resilience recovery benefit

Initialize $V(s) \leftarrow$ empty memorization table, $P(s) \leftarrow$ empty predecessor table
Function $V(s)$:
if $s = N_D$ **then return** 0
if $s \in V$ **then return** $V(s)$
Best_value$\leftarrow -\infty$, Best_node $\leftarrow$ null
for each $n \in N_D \setminus s$ **do**
$s^* \leftarrow s \cup \{n\}$
Current_value$\leftarrow g(s^*) + V(s^*)$
if Current_value > Best_value **then**
Best_value $\leftarrow$ Current_value, Best_node$\leftarrow n$
$V(s) \leftarrow$ Best_value, $P(s) \leftarrow$ Best_node
return $V(s)$
Main procedure:
$Z^* \leftarrow V(\varnothing)$, $\pi^* \leftarrow$empty list, $s \leftarrow \varnothing$
while $s \neq N_D$ **do**
$n \leftarrow P(s)$ append n to π^*, $s \leftarrow s \cup \{n\}$
Return π^* *and* Z^*

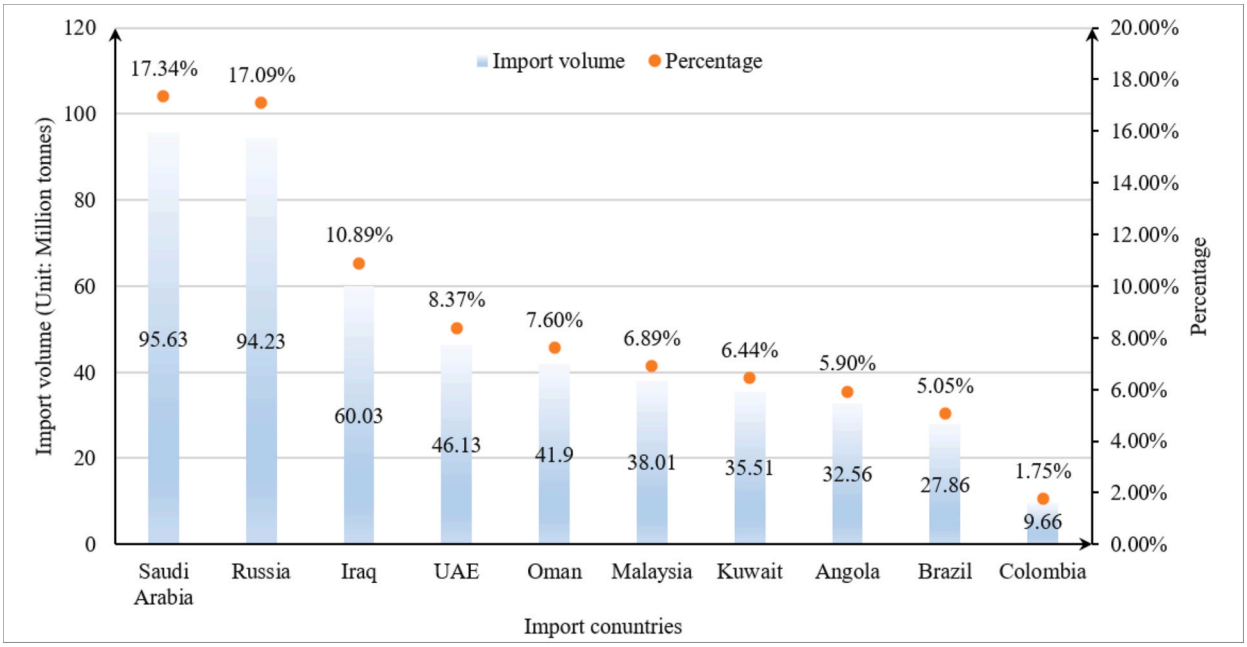

Fig. 4. China's maritime crude oil imports countries (from Jan 2022 to Dec 2023).

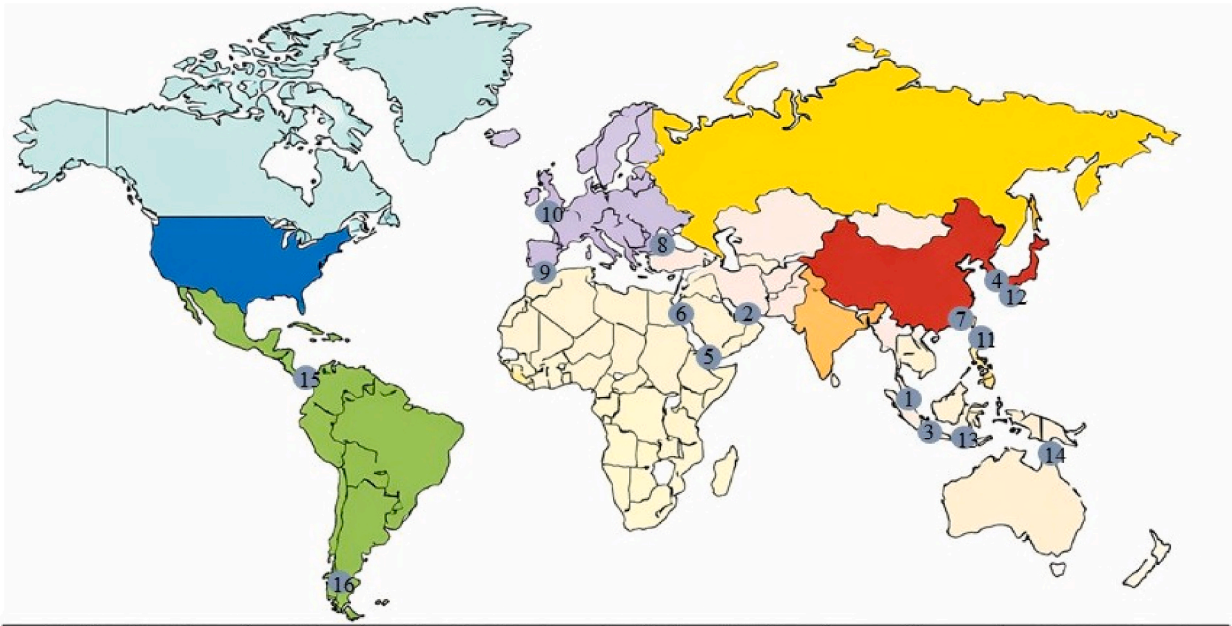

Maritime chokepoints	ID	Throughput (Tonnes)	Maritime chokepoints	ID	Throughput (Tonnes)
Malacca Strait	1	686346351	Strait of Gibraltar	9	15747000
Strait of Hormuz	2	396039600	English Channel	10	15746000
Sunda Strait	3	132466600	Bashi Channel	11	3676000
Korea Strait	4	101789396	Osumi Strait	12	2508911
Bab el-Mandeb Strait	5	59211000	Lombok Strait	13	2388000
Suez Canal	6	53433000	Torres Strait	14	1879000
Taiwan Strait	7	49210000	Panama Canal	15	1779000
Turkish Straits	8	17786000	Strait of Magellan	16	220000

Fig. 5. The critical maritime chokepoints among China's crude oil shipping network.

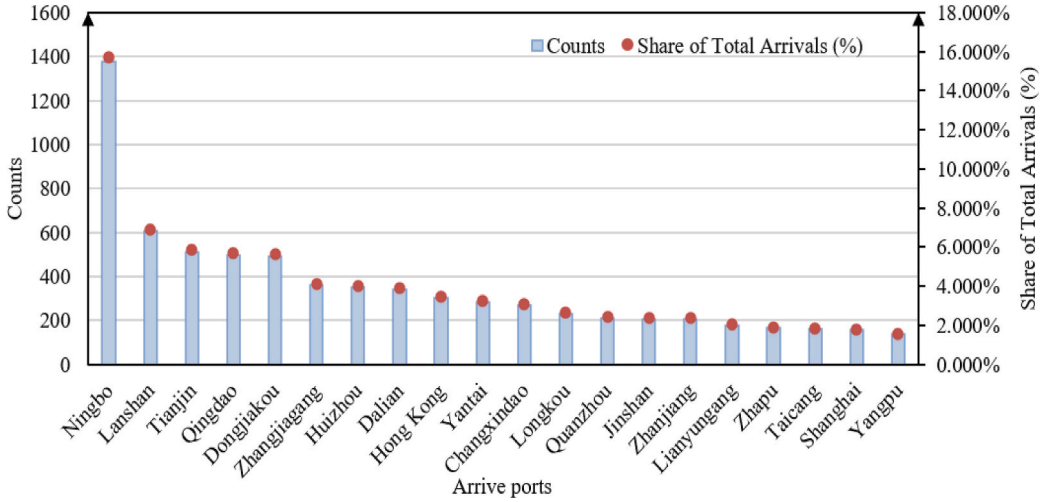

Fig. 6. Counts and relative shares of crude oil import ports in China.

Ningbo port and Lanshan port are the main entry points for Middle Eastern energy, Tianjin acts as a critical energy trade hub within the Asia-Pacific regional network.

As shown in Fig. 7, the distribution of shipping distances for crude oil routes is extremely uneven.

Most of the shipping distances are concentrated in two range groups, which are 1,000 to 1,500 Nautical Miles and 6,000 to 6,500 Nautical Miles. The shorter routes are mainly used for transport from the Kozmino port in Russia and Singapore port to Chinese coastal ports. In contrast, the longer routes between 6,000 and 6,500 Nautical Miles represent the primary supply lines from the Middle East. These routes connect major export hubs such as Ras Tanura in Saudi Arabia, Basrah in Iraq, Kuwait Port, and Mina Al Fahal in Oman to Chinese crude oil import terminals. This clear separation between short-range and long-range shipping routes highlights the different levels of maritime risk and the heavy reliance on long-distance energy corridors from the Middle Eastern area, which further highlights the critical role of Hormuz strait (No.2).

5.2. Resilience assessment results analysis

To demonstrate the effectiveness of the proposed framework, two extreme scenarios are simulated as baseline settings. These scenarios assess network resilience by considering different recovery priorities. The baseline settings are depicted in Table 6.

In Scenario 1, ε is set to 1, indicating that the recovery sequence is determined by prioritizing network-level resilience restoration. In Scenario 2, ε is set to 0, indicating that the recovery sequence is determined by prioritizing the node-level recovery priorities of disrupted maritime chokepoints. The recovery priority scores of maritime chokepoints are identified from a Rule-based Bayesian (RBN) network framework proposed by Fan et al., 2023. These scores represent relative resilience contribution of different maritime

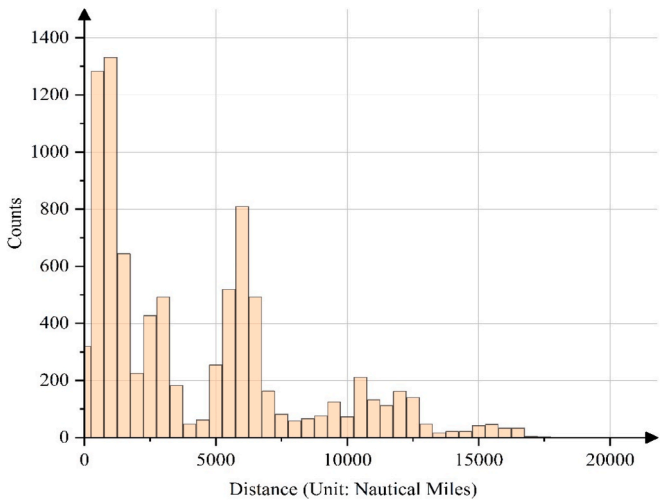

Fig. 7. Distance distribution of main crude oil shipping routes to China.

chokepoints. In this study, they are employed as node-level recovery priority parameters during the resilience restoration stage, the detailed information could be found in the Appendix A.

The value of α is determined based on the empirical distribution of shipping distances in China's crude oil shipping network shown in Fig. 7. Based on the AIS voyage database containing 9,138 crude oil transportation voyages, the median sailing distance is 5,295 nautical miles and the average distance is 5,962 nautical miles. Fig. 7 also shows that most shipping routes are concentrated within several major distance intervals, indicating that disruptions at maritime chokepoints usually result in moderate increases in transportation distance rather than unlimited detours. Therefore, the selected range of α provides a realistic representation of different levels of alternative routing capability and is suitable for conducting sensitivity analysis under diverse disruption scenarios.

The corresponding resilience trends are depicted in Fig. 8 (a) and Fig. 8 (b), respectively. The comparative results derived from Scenarios 1 and 2 demonstrate that the recovery priority parameter ε significantly influences the resilience restoration performance of China's crude oil shipping network. It is worth mentioning that, during the recovery simulation process, each recovery node decision step corresponds to the restoration of exactly one disrupted chokepoint. Accordingly, the number of restored nodes increases by one after each recovery step. In this study, since each recovery step is assumed to have an equal duration, the area-based resilience metric captures the cumulative transportation capacity throughout the recovery process. Therefore, delayed recovery is reflected in the resilience assessment through the additional transportation capacity loss accumulated during the remaining recovery steps. However, when network performance approaches its baseline level, the additional penalty associated with the remaining recovery steps becomes relatively small.

Table 7 shows the simulation results under different scenarios. As shown in Fig. 8, during the degradation phase from the first seven maritime chokepoints, both scenarios exhibit identical performance declines because the disruption sequences remain consistent. However, a clear divergence emerges during the recovery phase. As shown in Fig. 8, when ε equals 1.0, the network achieves a complete recovery more rapidly than in Scenario 2. For instance, at a threshold of 0.1, Scenario 1 requires only 14 nodes to reach full performance. In contrast, Scenario 2 necessitates 16 nodes to achieve the same outcome. This finding demonstrates that prioritizing network-level resilience restoration strategy can accelerate the recovery process and reduce cumulative resilience losses. Delving into specific data points at the 0.1 threshold, Scenario 1 reaches a performance level of 0.971 by the 13th node restoration. Although Scenario 2 shows a high value of 0.999 at the same stage, its overall trajectory involves more nodes to resolve the final performance gaps across different thresholds. As the alternative routing capability increases to 0.5, the advantage of the network-level resilience restoration strategy in Scenario 1 becomes even more pronounced. Under this setting, the network completes its recovery at the 15th node, whereas Scenario 2 lags behind in the intermediate stages of restoration. While Scenario 2 prioritizes the node-level recovery priorities of disrupted maritime chokepoints, this strategy results in a longer restoration trajectory under severe disruption conditions. Under the node-level recovery priorities of disrupted maritime chokepoints strategy, the restoration process may require more time, thereby resulting in greater cumulative resilience losses. Therefore, when rapid system restoration is highly required, decision-makers should prioritize maritime chokepoints that contribute most to network-level resilience restoration, thereby minimizing cumulative resilience losses and accelerating the recovery peace to a stable operating state.

The alternative routing capability parameter in this study represents the flexibility of rerouting cargo flows under maritime chokepoint disruption scenarios. A higher threshold implies a greater availability of alternative paths within the shipping network, which fundamentally strengthens the system's inherent resilience and mitigates cargo flow losses. As the threshold increases from 0.1 to 0.5, the degradation phase shows a more gradual performance decline. Specifically, with a threshold of 0.5, the system maintains a performance level of 0.796 under the disruption of the first node (Strait of Hormuz), whereas it drops sharply to 0.465 at a 0.1 threshold. Additionally, under the high alternative routing capability scenario ($\alpha = 0.5$), the resilience curve approaches zero only after the failure of 8 key nodes. In contrast, when $\alpha = 0.1$, the crude oil shipping network becomes fully disrupted with the loss of only five key nodes. This disparity confirms that enhanced route redundancy allows the network to absorb shocks more effectively by rerouting cargos through substitute maritime chokepoints. Consequently, the resilience fluctuations in the degradation phase shrinks as the threshold rising, reflecting a direct reduction in cumulative economic impact.

Furthermore, the impact of recovery priority parameter ε is closely relies on the level of alternative routing capability. At lower thresholds of ε, where alternative options are limited, prioritizing network-level resilience restoration ($\varepsilon = 1$) becomes particularly important. However, as the threshold reaches 0.5 and the network becomes more flexible, prioritizing the node-level recovery priorities of disrupted maritime chokepoints ($\varepsilon = 0$) becomes increasingly competitive. In highly redundant network structure, the abundance of alternative routes diminishes the urgency of restoring specific critical nodes. These findings suggest that the recovery preference represented by ε should be dynamically adjusted according to the available alternative routing capability and the disruption dynamics.

Table 6
Baseline parameter settings and descriptions.

Parameter	Value set	Description
ε	0, 1	Resilience recovery priority parameter.
α	0.1, 0.3, 0.5	Alternative routing capability parameter.
β	8	Maximum number of disrupted maritime chokepoints during the disruption phase.

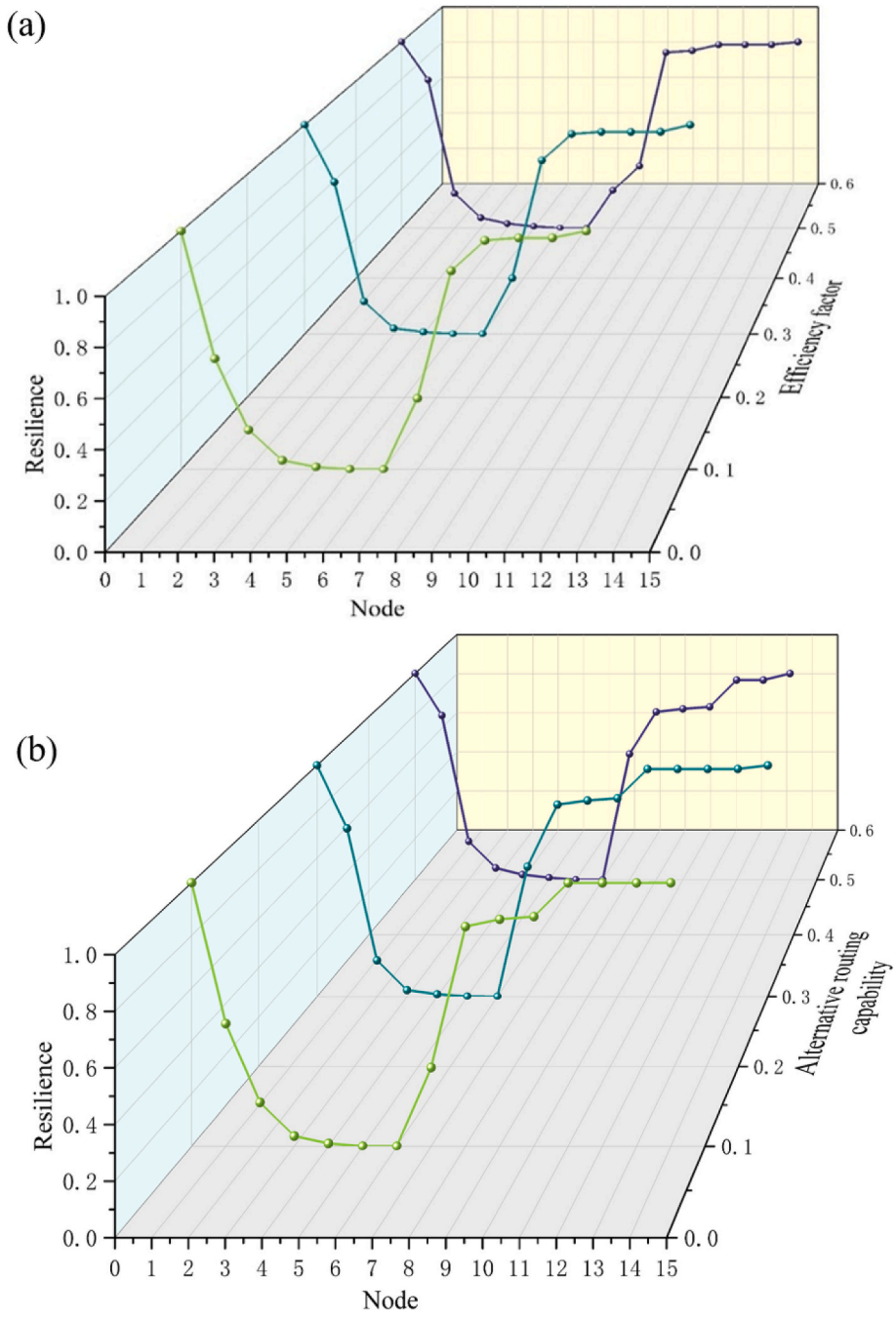

Fig. 8. Resilience index curves under multiple optimization methods considering various recovery priorities.

5.3. Resilience comparative analysis considering the alternative capabilities variation

Fig. 9 and Fig. 10 are demonstrate the resilience loss over recovery phases and total resilience index differences across alternative route capabilities upon maritime chokepoints under disruptions, respectively.

The comparative experiments reveal that recovery preference is highly relevant to the alternative routing capabilities. As shown in Fig. 9, under the low alternative routing capability ranging from 0.1 to 0.2, Scenario 1 consistently yields a lower total loss compared to Scenario 2. Notably, when α=0.20, the recovery loss in Scenario 1 is 0.945, which is approximately 25% lower than the value of 1.259 observed in Scenario 2. These findings indicate that when feasible alternative routes are limited, prioritizing network-level resilience restoration strategy is essential for rapidly recovering China's crude oil shipping network and minimizing cumulative resilience losses.

Table 7
Parameter setting and the results obtained from the optimization-based framework.

Parameter setting	Alternative routing capability parameter	Disruption sequence	Recovery sequence
$\varepsilon = 1$	$\alpha = 0.1$	2, 1, 4, 3, 7, 5, 9	1, 2, 4, 7, 6, 9, 5
	$\alpha = 0.3$		2, 1, 4, 7, 6, 9, 5, 3
	$\alpha = 0.5$		2, 1, 4, 7, 6, 9, 5, 3
$\varepsilon = 0$	$\alpha = 0.1$	2, 1, 4, 3, 7, 5, 10	1, 5, 3, 2, 4, 6, 7, 9, 10
	$\alpha = 0.3$		1, 5, 3, 2, 4, 6, 7, 9, 10
	$\alpha = 0.5$		1, 5, 3, 2, 4, 6, 7, 9, 10

However, as α increases from 0.3 to 0.5, Scenario 2 demonstrates superior performance by achieving lower cumulative resilience losses. For instance, when α=0.4, Scenario 2 reduces the recovery loss to 1.066, a significant improvement over Scenario 1's 1.774. This suggests that under a highly redundant shipping network structure, priorities of disrupted maritime chokepoints show increasingly beneficial. The abundance of alternative routes reduces the urgency of restoring specific critical maritime chokepoints, allowing the network to maintain an acceptable resilience levels while adopting a more flexible restoration strategy.

In contrast, Fig. 10 shows that the total resilience loss under various values of α. Fig. 9 and Fig. 10 reveal that the degradation losses remain identical for both scenarios under each value of α. This finding provides empirical evidence that the absorptive capacity of the system is independent from the subsequent recovery strategies. Instead, the initial impact of a disruption is determined solely by the network topology and the inherent substitutability of the maritime routes. This finding allows decision-makers to decouple the assessment of immediate network vulnerability from the long-term planning of restoration efforts.

Additionally, a sensitivity analysis was conducted to illustrate the interactions between alternative routing capability and the recovery strategy preferences. Fig. 11 and Fig. 12 show the resilience losses during the recovery phase and the total resilience losses under 55 experimental combinations. Interestingly, Fig. 11 shows a non-linear relationship between the recovery losses and the alternative routing capability of the maritime chokepoints. It could be found that when α increases from 0.10 to 0.20, the recovery loss decreases from 1.038 to 0.945, indicating that a moderate increase in alternative routes' feasibility enhances the recovery effectiveness. However, as α increases from 0.20 to 0.50, the overall resilience loss during the recovery stage gradually increases to 2.212. This possibly attributes to the changing role of critical maritime chokepoints under different network structures. When alternative routing capability is limited, the network relies on a small number of the critical maritime chokepoints, making the rapid recovery of failed nodes highly beneficial. However, with a highly redundant network structure, disrupted cargo flows could be rerouted through various alternative paths, reducing the urgency of recovering the critical failed nodes. Consequently, the marginal benefits of recovering the critical chokepoints gradually diminish, leading to increased cumulative recovery losses. These findings suggest that improving alternative route capability alone cannot solely reduce recovery losses, thereby network redundancy and recovery resource allocation should be balanced in real-world practice.

Fig. 12 further enhances these findings, showing that the lowest resilience loss occurs when α=0.40 and ε=0.0, indicating that prioritizing node-level recovery strategy becomes more effective when alternative routing capability is sufficient. This finding also suggests that a higher level of alternative routing capability is not always associated with lower resilience losses. Under certain conditions, excessive reliance on network-level resilience restoration may prolong the restoration process and rise the overall resilience loss from a system optimization perspective.

5.4. Comparison analysis on resilience assessment under different recovery strategies

In this study, four traditional centrality-based attack strategies, including the degree centrality, betweenness centrality, closeness centrality, and PageRank index are employed to benchmark the proposed optimization-based framework. It should be noted that these

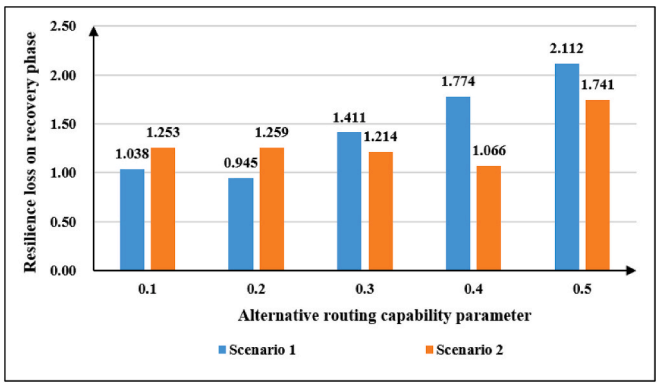

Fig. 9. Recovery loss under different alternative routing capability parameters.

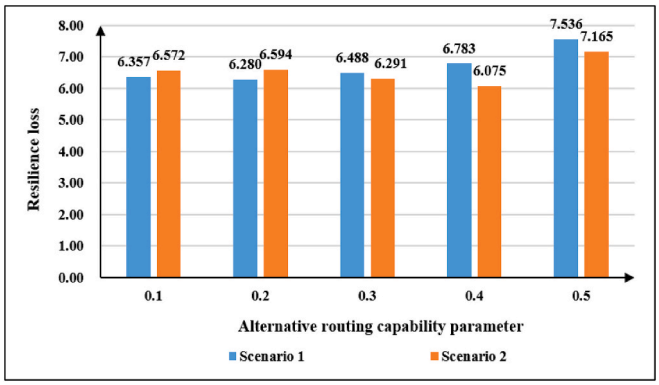

Fig. 10. Cumulative resilience loss under different alternative routing capability parameters.

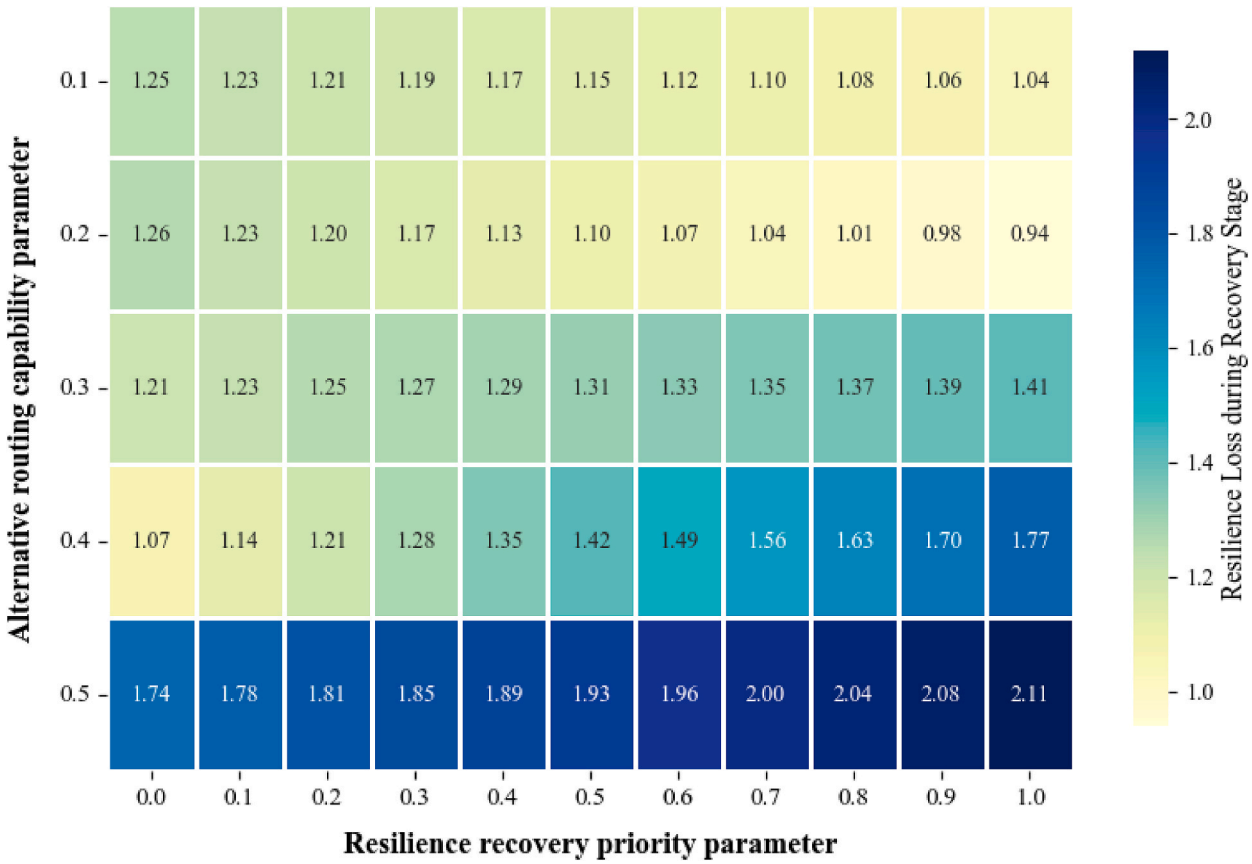

Fig. 11. Sensitivity analysis on recovery loss under different scenarios.

centrality-based attack strategies aim to identify the structurally critical maritime chokepoints based on the static network structure, whereas the proposed framework focuses on identifying the disruption sequence that induces the maximum cumulative resilience loss from a system-level perspective. Therefore, the comparative analysis is conducted to highlight vulnerability assessment from diversity perspective and to verify the capability of the proposed framework in identifying worst-case disruption scenarios and optimal recovery sequences for China's crude oil shipping network. The nodes identified by these metrics are prioritized within the disruption and recovery sequences, and the detailed results are summarized in Table 8.

As illustrated in Fig. 8, the removal of at most 8 critical nodes leads to a complete system collapse, reducing the overall resilience performance to zero. To ensure baseline consistency, the 8 nodes ranked highest from different centrality-based indexes are selected as candidate nodes for the comparative analysis. As shown in Fig. 13, four typical scenarios are designed for empirical investigation, characterized by different parameter settings: where (a), $\varepsilon = 1.0$ and α=0.1; (b) $\varepsilon = 0.0$ and α=0.1; (c). $\varepsilon = 1.0$ and α= 0.5; and finally

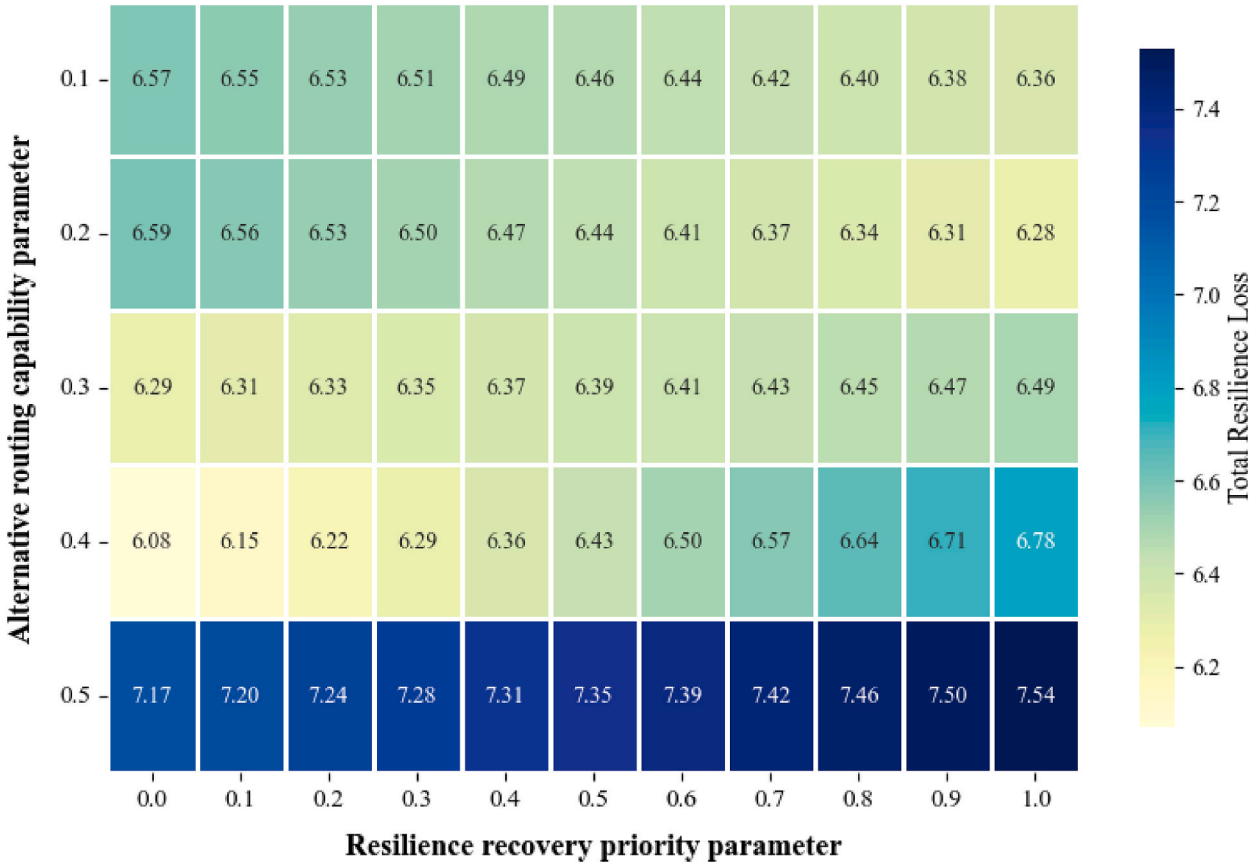

Fig. 12. Sensitivity analysis on total resilience loss under different scenarios.

(d) $\varepsilon = 0.0$ and α=0.5.

The resilience losses are calculated by Equation (1). The total resilience loss, degradation resilience loss, and recovery resilience loss are presented in Fig. 14. Across all simulated scenarios, Strategy 1 exhibits better resilience restoration performance under scenarios with limited alternative routing capability. From a strategic optimization perspective, under conditions of limited alternative routing capability, prioritizing network-level resilience restoration ($\varepsilon = 1$) serves as the primary mechanism for mitigating resilience losses and accelerating system restoration. Conversely, under conditions of high alternative capability, prioritizing the node-level recovery priorities of disrupted maritime chokepoints ($\varepsilon = 0$) may achieve lower cumulative resilience losses through more flexible restoration pathways. This finding emphasizes that resilience performance should not be evaluated solely by delaying system collapse, but also by the effectiveness of post-disruption resilience restoration.

Additionally, the empirical results shown in Fig. 13 reveal a critical resilience restoration threshold. under severe disruption scenarios, all recovery preferences except Strategy 1 fail to restore the network resilience beyond a performance level of 0.70. This finding suggests that disruptions at major maritime chokepoint may not only reduce network resilience performance in the short term but may also prevent the network from fully recovering to its pre-disruption state.

Table 8
Comparison of disruption and recovery sequence based on different strategies.

No.	Strategy	Ranking results	Strategy explanation
1	Optimization Method	–	The nodes after optimization methods are prioritized within disruption and recovery sequences.
2	Degree centrality	[1, 2, 3, 4, 5, 6, 7, 8, 9, 10, 11, 12, 13, 14, 15, 16]	The nodes with a higher number connection with other nodes are prioritized within disruption and recovery sequences.
3	Between centrality	[10, 8, 9, 6, 5, 2, 1, 4, 12, 3, 7, 14, 13, 15, 11, 16]	The nodes act as intermediaries on the shortest paths between other nodes are prioritized within disruption and recovery sequences.
4	Closeness centrality	[1, 4, 5, 6, 7, 2, 12, 9, 14, 10, 8, 3, 15, 13, 11, 16]	Nodes with higher proximity to all other nodes are prioritized within disruption and recovery sequences.
5	PageRank index	[1, 2, 4, 7, 3, 6, 5, 10, 8, 9, 15, 12, 14, 13, 11, 16]	Nodes receive links from other highly influential or well-connected nodes are prioritized within disruption and recovery sequences.

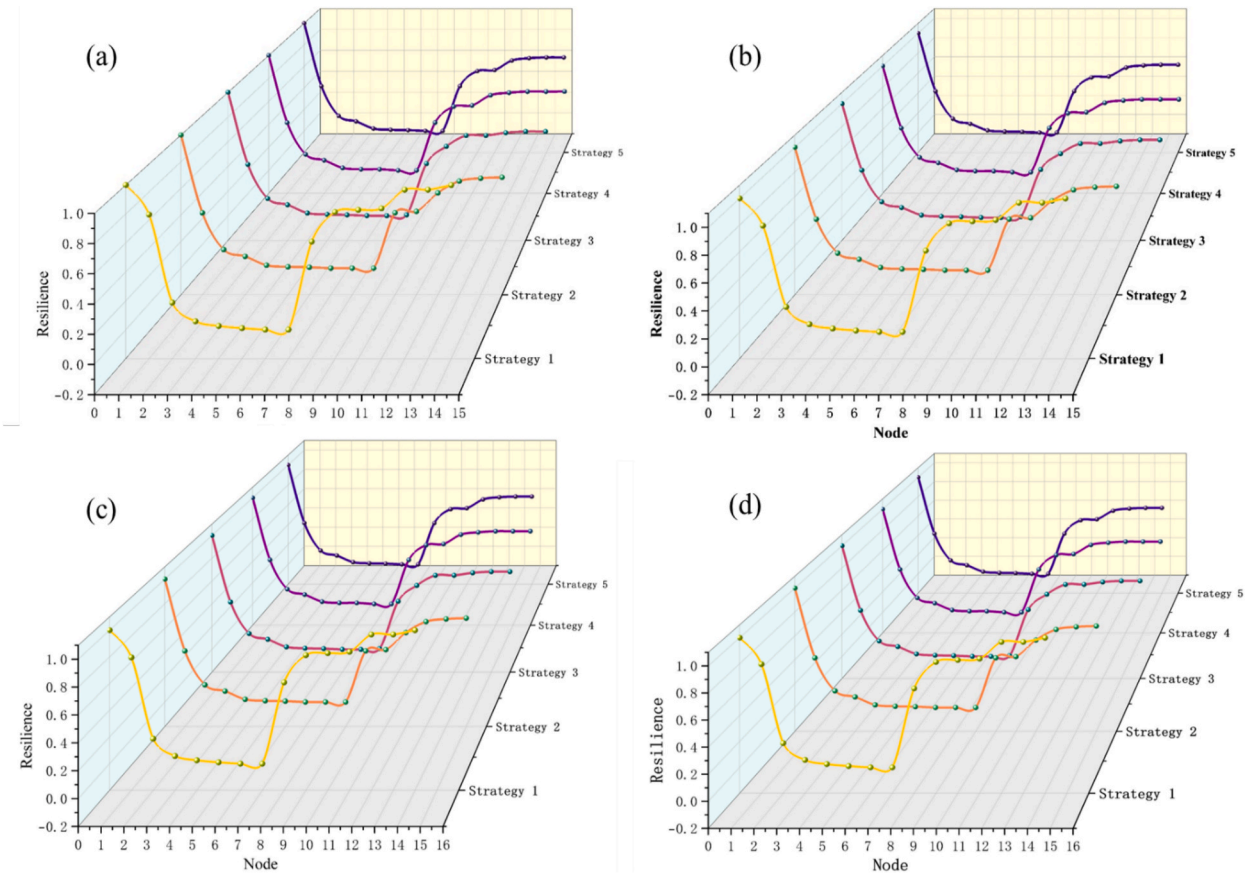

Fig. 13. Resilience assessment curves under different strategies. (a), $\varepsilon = 1.0$ and $\alpha = 0.1$; (b) $\varepsilon = 0.0$ and $\alpha = 0.1$; (c). $\varepsilon = 1.0$ and $\alpha = 0.5$; and finally (d) $\varepsilon = 0.0$ and $\alpha = 0.5$.

Following findings are derived by analyzing characteristics of resilience loss. Firstly, in degradation phase, Strategy 4 exhibits the highest level of stability, whereas Strategy 1 demonstrates greater fluctuations in resilience performance. This divergence illustrates a significant difference, where Strategy 1 deliberately prioritizes radical systemic reconfiguration over immediate performance retention, effectively conceding short-term robustness to secure an accelerated and total recovery after external disruptions. Secondly, regarding that recovery stage contributes more than 60% of the total resilience loss variance, Strategy 1 emerges as the superior practice despite its initial instability. Conversely, Strategy 3 is identified as the most precarious configuration due to its high volatility at 1.192. Under extreme perturbations, Strategy 3 exhibits a tendency to transition from temporary impairment to permanent paralysis, representing a critical failure mode that maritime authorities must mitigate to ensure long-term maritime chokepoints security.

In the comparative analysis experiments, although our proposed optimization-based recovery strategy demonstrates better resilience performance than four centrality-based strategies under most scenarios, this advantage should be considered alongside the computational resources and timing constraints of different approaches. Specifically, the optimization-based framework involves solving a combinatorial decision-making problem, which may incur substantial computational costs as the number of disrupted maritime chokepoints and feasible alternative routing increases. In contrast, centrality-based strategies primarily rely on network topological information and generally require less computational effort, enabling faster identification of recovery strategy priorities. Hence, from a practical perspective, the selection of decision -making strategies should consider from computational resources, emergency response timing constraints, and the complexity of real-world scenarios. Specifically, optimization-based strategies are suitable for strategic resilience planning and recovery resource allocation, where computational time constraint is relatively available. Centrality-based strategies are more suitable for time-sensitive emergency response, where rapid decision-making is essential.

6. Discussions and analysis

This section discusses the research findings from three critical perspectives to bridge the gap between simulation experiments and practical applications. Finally, we provide policy implications to help decision-makers to enhance the resilience performance for maritime energy shipping network.

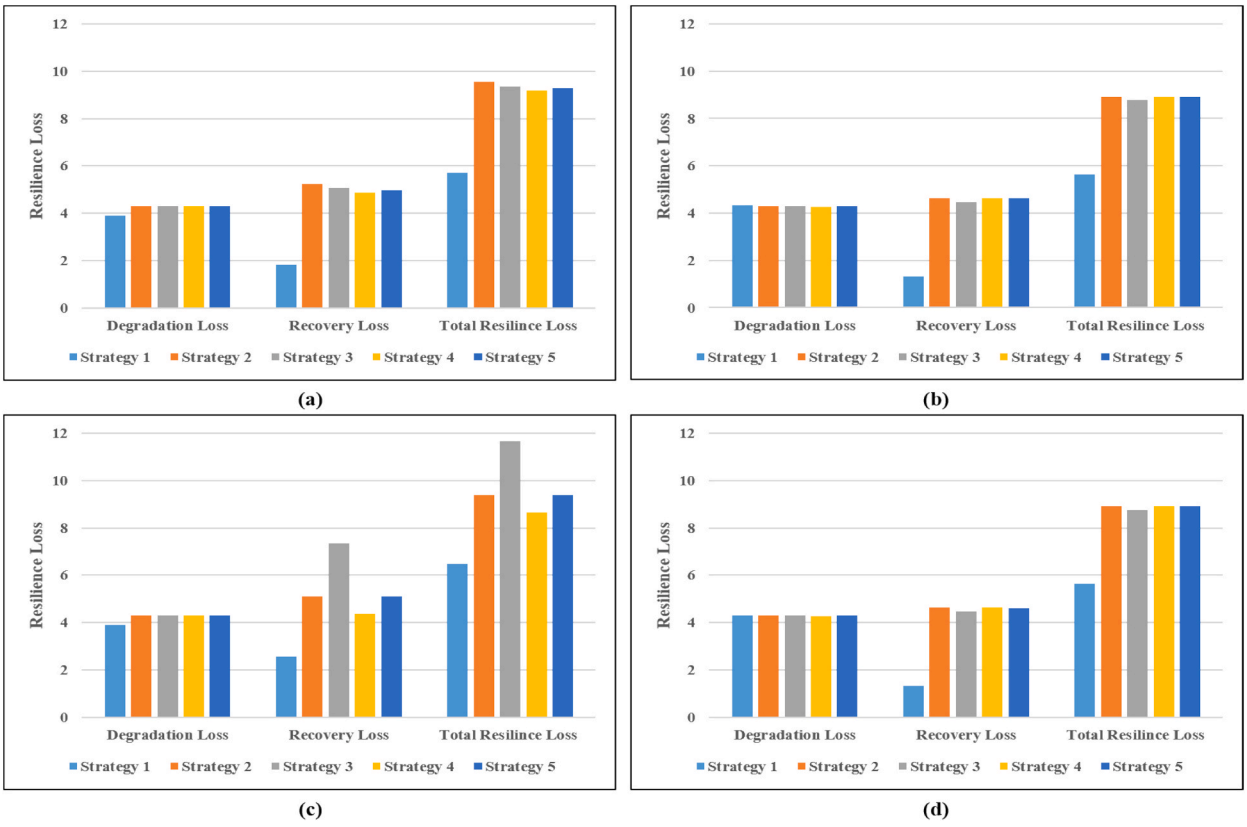

Fig. 14. Resilience loss under different strategies.

6.1. *Resilience boundaries revealed by worst-case disruption scenario analysis*

Beyond identifying critical maritime chokepoints, this study highlights the importance of worst-case disruption analysis for maritime transportation systems. Conventional vulnerability assessments often rely on random failure simulations or centrality-based attack strategies, which may underestimate the systemic risks associated with cascading disruptions. By explicitly searching for the worst-case disruption pathway, the proposed framework identifies the resilience boundary of China's crude oil shipping network.

The results show that the network performance can deteriorate rapidly once disruptions occur at a small number of critical chokepoints. This finding underscores the structural dependence of the global crude oil shipping network on a limited number of maritime corridors. In response, the proposed framework functions as a stress-testing tool, allowing decision-makers to evaluate how quickly network performance may decline under extreme scenarios and to identify the most severe resilience degradation pathways.

Furthermore, the analysis reveals that the alternative capability of critical nodes exhibits a non-linear relationship with resilience losses incurred in the recovery phase. At relatively low levels of alternative routing capability, preventing effective rerouting due to chokepoints failures and leading to substantial initial losses. As the alternative routing capability parameter increases, more alternative paths become available, enabling cargo flows to be redistributed. However, excessive routing flexibility may also prolong the resilience restoration process and increase cumulative resilience losses during the recovery stage. Therefore, decision-makers should carefully balance network-level resilience restoration and node-level recovery priorities when designing resilience restoration strategies under various disruption scenarios.

6.2. *Strategic importance of maritime chokepoints under geopolitical risks*

The simulation results consistently identify the Strait of Hormuz, the Malacca Strait, the Korea Strait, and the Taiwan Strait as critical nodes within China's crude oil shipping network. Among these, the Strait of Hormuz plays the most dominant role in determining overall network resilience. Approximately 40–55% of China's crude oil imports pass through this corridor, and major suppliers such as Saudi Arabia and Iraq rely heavily on this route to access Asian markets.

These findings are consistent with the "Rich Club" phenomenon observed in global crude oil trade networks, where a small group of major trading countries and strategic corridors dominate the global energy supply structure (Niu et al., 2023). As a result, disruptions affecting these key chokepoints may trigger cascading effects across the broader shipping network.

Recent geopolitical developments further underscore the practical relevance of this analysis. In early 2026, escalating military

confrontations between the United States and Iran led to severe disruptions in the Strait of Hormuz, one of the most critical maritime chokepoints in the global energy transportation network. Following a series of U.S. and Israeli strikes on Iranian military and energy infrastructure, Iranian authorities announced restrictions on maritime transit through the strait, causing tanker traffic to drop sharply and leading to a near halt in oil shipments[4]. Reports indicate that shipping activity passing the Strait of Hormuz declined by more than 70%, with some periods seeing almost no vessels transiting the strait. However, as approximately 20% of global oil supply normally passes through this corridor, the disruption triggered a surge in global oil prices and widespread concerns regarding energy supply security[5]. These real-world developments illustrate the type of extreme geopolitical shock scenarios considered in this study and highlight the importance of worst-case disruption analysis and resilience stress testing for critical maritime chokepoints.

In comparison, the Malacca, Korea, and Taiwan Straits primarily function as intermediate chokepoints for crude oil imports. The Malacca Strait exhibits relatively high redundancy because nearby alternatives such as the Sunda and Lombok Straits provide geographically feasible substitutes (Fan et al., 2023). Although the Korea and Taiwan Straits have fewer alternative routes, their proximity to the Chinese mainland offers logistical advantages. In the event of disruptions, vessels can be rerouted to these areas with relatively limited additional transportation distances.

6.3. Recovery strategy prioritization for enhancing resilience performance

Based on our results from Section 5.3, the recovery optimization analysis indicates that the Strait of Malacca, the Strait of Bab el-Mandeb, the Sunda Strait, and the Strait of Hormuz consistently emerge as primary recovery nodes under the node-level recovery priority preference strategy. Notably, the Malacca Strait demonstrates particularly strong resilience restoration capability. Although it is the most congested maritime corridor globally, its resilience benefits from robust institutional coordination among the littoral states of Indonesia, Malaysia, and Singapore.

Since the early 2000s, these countries have established cooperative security and monitoring mechanisms to address maritime threats in the region. The launch of the Malacca Straits Patrol (MSP) initiative in 2004 including joint patrols, 24-hour communication channels, and real-time intelligence sharing, significantly improving the region's ability to respond to maritime disruptions (Fan et al., 2023). These institutional arrangements enable rapid operational coordination and contribute to the rapid recovery of shipping activities following external disturbances.

The results therefore suggest that institutional resilience plays an important role alongside physical infrastructure in enhancing network recovery efficiency. Effective governance mechanisms, regional cooperation frameworks, and coordinated emergency response systems can substantially improve the resilience performance of critical maritime corridors.

6.4. Policy implications

The proposed framework provides a unified analytical tool for evaluating the vulnerability and resilience recovery capacity of crude oil shipping networks using high quality AIS-based maritime big data. By jointly considering network-level resilience restoration and node-level recovery priorities of disrupted maritime chokepoints, the framework captures the trade-offs that characterize resilience restoration strategies decision-making in maritime transportation systems.

Importantly, the results suggest that enhanced alternative routing capability does not necessarily lead to proportional improvements in overall network resilience. While additional routing options can reduce immediate disruption impacts, excessive redundancy may increase transportation distance, shipping costs, and emissions. Moreover, excessive flexibility may extend the recovery process and increase cumulative resilience losses. These findings reveal a diminishing return effect in resilience investment, indicating that optimal resilience strategies should focus on achieving a balanced trade-off among redundancy, efficiency, and cost.

It is also worth noting that the alternative route capability is not static in real-world maritime shipping networks. Although some of the alternative routes could be theoretically available, they may become infeasible due to the dynamic conditions such as the geopolitical conflicts, climate change, and adverse weather conditions. Consequently, the decision-makers should continuously update the real alternative routes derived from real-world AIS trajectories, port congestion scores, and geopolitical risk alarms. Such a dynamic adjustment mechanism enables decision-makers to avoid relying on a fixed recovery preference, instead of employing resilience restoration priorities according to evolving operational conditions. This adaptive approach can further enhance the resilience of crude oil shipping networks and improve the effectiveness of emergency response and resources planning.

Although this study focuses on crude oil transportation, the proposed framework is highly adaptable and can be extended to other strategic commodity networks, such as dry bulks transportation systems. By integrating worst-case disruption analysis with recovery optimization, the framework offers a practical tool for supporting global supply chain security and strategic resources management under increasing geopolitical conflicts and environmental uncertainties.

7. Conclusions

Motivated by geopolitical disruptions and the potential closure of maritime chokepoints, this study proposes an optimization-based framework to assess the resilience of the crude oil shipping network. Using China's crude oil shipping network as a case study,

[4] https://www.bloomberg.com/news/articles/2026-03-12/strait-of-hormuz-how-is-iran-war-disrupting-oil-trade-can-naval-escorts-help
[5] https://www.reuters.com/business/energy/barclays-raises-2026-brent-forecast-85-barrel-strait-hormuz-disruption-2026-03-13/

employing real-world AIS-based maritime big data, this study provides a comprehensive understanding of crude oil trade dynamics and shipping voyage details. Different from previous studies that rely on centrality-based metrics for targeted attacks on critical nodes, our approach identifies the worst-case scenarios from the perspective of node failure sequences. During the recovery phase, the proposed framework jointly considers network-level resilience restoration and node-level recovery priorities of disrupted maritime chokepoints, thereby providing a more realistic resilience restoration assessment.

(1) A non-linear relationship is observed between resilience losses and the alternative capability of maritime chokepoints.

(2) For decision-makers prioritizing node-level recovery priorities, the ideal alternative route capability is around 0.40. In contrast, for those prioritizing network-level resilience restoration, the ideal level is 0.20. Our findings confirm that when chokepoints are blocked, re-routing is not always the best solution. Instead, focusing on recovering the critical chokepoints can be more beneficial than simply using longer shipping routes.

(3) Our framework provides a more effective identification of worst-case disruption scenarios and resilience restoration strategies than traditional centrality-based approaches.

Finally, we suggest several directions for future research. Firstly, although our current database covers two years of data, a larger dataset would allow for a more dynamic resilience analysis. Additionally, this study does not include crude oil imported by pipeline transport. Future research could incorporate pipeline transport as an alternative option to analyze network resilience under different external disruption scenarios.

Secondly, this study focuses on the Chinese crude oil shipping network. Since different countries have diverse trade patterns, shipping routes, and maritime chokepoints, the topological characteristics of their shipping networks will be presented in a different form. Therefore, future studies are encouraged to apply the proposed framework to other national or regional shipping networks to examine its broader applicability and enhance its generality. Thirdly, the proposed framework assumes that the alternative routes selection is primarily determined by sailing distance. In practice, the feasibility of alternative routes is also influenced by the insurance premiums, geopolitical risks, fuel price fluctuations, and the costs associated with passing through the critical maritime chokepoints. Additionally, the alternative routes may suffer from the capacity bottlenecks during the large-scale congestion, climate change conditions, and others. Consequently, future studies could construct and incorporate dynamic cost structures and capability-constrained network models to better capture the real-world operational conditions and expand the theoretical scope of the proposed framework. Fourthly, this study adopts a binary disruption-state representation of maritime chokepoints to identify the resilience boundary of the crude oil shipping networks for simulating the scenarios where the access to the chokepoints is fully lost. Future research may extend the proposed framework by incorporating multi-state disruption mechanisms to represent different levels of maritime chokepoint degradation, such as partial throughput reductions caused by congestion, adverse weather conditions and others. Additionally, the dynamic disruption propagation mechanisms could be introduced to capture the spatial-temporal cascading effects among interconnected maritime chokepoints. Finally, the quantification of geopolitical risks could be a valuable extension. Since maritime chokepoints are often located in sensitive regions, future models could include a dynamic geopolitical risk index to predict potential disruptions more accurately. This would allow for a proactive resilience assessment rather than a reactive one, helping stakeholders better prepare for sudden regional conflicts or policy changes.

CRediT authorship contribution statement

Hanwen Fan: Writing – review & editing, Writing – original draft, Visualization, Validation, Methodology, Formal analysis, Data curation, Conceptualization. **Lingye Zhang:** Writing – review & editing, Resources, Methodology, Conceptualization. **Zhenming Wu:** Writing – review & editing, Writing – original draft, Visualization, Resources, Formal analysis, Data curation. **Haiying Jia:** Writing – review & editing, Writing – original draft, Resources, Data curation, Conceptualization. **Zaili Yang:** Writing – review & editing, Writing – original draft, Visualization, Validation, Supervision, Resources, Project administration, Methodology, Funding acquisition.

Declaration of competing interest

The authors declare that they have no known competing financial interests or personal relationships that could have appeared to influence the work reported in this paper.

Acknowledgement:

This project has received funding from the European Research Council (ERC) under the European Union's Horizon 2020 research and innovation programme (Grant Agreement No. 864724)

Appendix

Appendix A. . Resilience Scores of Maritime Chokepoints.

Maritime chokepoints	Resilience score
Malacca Strait	0.641
Strait of Hormuz	0.545
Sunda Strait	0.547
Korea Strait	0.638
Bab el-Mandeb Strait	0.533
Suez Canal	0.608
Taiwan Strait	0.670
Turkish Straits	0.639
English Channel	0.477
Strait of Gibraltar	0.579
Bashi Channel	0.592
Osumi Strait	0.545
Lombok Strait	0.569
Torres Strait	0.500
Panama Canal	0.628
Strait of Magellan	0.500

Data availability

The authors do not have permission to share data.

References

Bai, X., Ma, Z., Zhou, Y., 2023. Data-driven static and dynamic resilience assessment of the global liner shipping network. Transportation Research Part e: Logistics and Transportation Review 170, 103016.

Bei, X., Zhu, X., Coit, D.W., 2019. A risk-averse stochastic program for integrated system design and preventive maintenance planning. Eur. J. Oper. Res. 276, 536–548.

Calatayud, A., Mangan, J., Palacin, R., 2017. Vulnerability of international freight flows to shipping network disruptions: a multiplex network perspective. Transportation Research Part e: Logistics and Transportation Review 108, 195–208.

Cao, Y., Xin, X., Jarumaneeroj, P., Li, H., Feng, Y., Wang, J., Wang, X., Pyne, R., Yang, Z., 2025a. Data-driven resilience analysis of the global container shipping network against two cascading failures. Logistics and Transportation Review, Transportation Research Part E, p. 193.

Cao, Y., Xin, X., Wang, X., Wang, J., Yang, Z., 2025b. Multi-objective resilience-oriented optimisation for the global container shipping network against cascading failures. Transp. Res. A Policy Pract. 200, 104659.

Chen, J., Jiang, H., Xu, J., Pang, C., Shi, J., Tan, Z., 2025. Resilience analysis from the perspective of global container shipping network evolution: Fine-grained modeling based on AIS data. J. Transp. Geogr. 129, 104415.

Dong, G., Qing, T., Du, R., Wang, C., Li, R., Wang, M., Tian, L., Chen, L., Vilela, A.L.M., Stanley, H.E., 2020. Complex network approach for the structural optimization of global crude oil trade system. J. Clean. Prod. 251, 119366.

Ducruet, C., Notteboom, T., 2012. The worldwide maritime network of container shipping: spatial structure and regional dynamics. Global Netw. 12, 395–423.

Fan, S., Yang, Z., Wang, J., Marsland, J., 2022. Shipping accident analysis in restricted waters: lesson from the Suez Canal blockage in 2021. Ocean Eng. 266, 113119.

Fan, H., Gong, X., Lyu, J., 2023. Resilience assessment of strait/canal: a rule-based Bayesian network framework. Transp. Res. Part D: Transp. Environ. 124, 103960.

Fan, H., Jia, H., Gong, X., Chang, Z., Lyu, J., 2026a. A Novel Framework for Quantitative Evaluation of Resilience Performance of Sea Lanes of Communication. Risk Anal. 46, e70274.

Fan, H., Jia, H., Wu, Z., 2026b. Natural disaster risks in seaports for global petroleum trades. Transportation Research Part e: Logistics and Transportation Review 210, 104784.

FOLKE, C., CARPENTER, S. R., WALKER, B., SCHEFFER, M., CHAPIN, T. & ROCKSTRöM, J. 2010. Resilience Thinking Integrating Resilience, Adaptability and Transformability. *Ecology and Society,* 15.

Fuentes, G., Munim, Z.H., 2025. Climate influence on Panama Canal operations: predicting canal water times with integrated environmental and operational data. Transportation Research Part e: Logistics and Transportation Review 203, 104319.

Gu, B., Liu, J., 2025. A systematic review of resilience in the maritime transport. Int J Log Res Appl 28, 257–278.

Hu, W., Shi, J., Pang, C., Chen, J., Wan, Z., Wang, Z., 2026. Assessment and optimization of shipping network resilience in the maritime silk road regions. J. Transp. Geogr. 130, 104454.

Ilyas, M., Jin, Z., Ullah, I., Almujibah, H., 2024. A fuzzy logic-based risk assessment framework for the crude oil transportation supply chain. Ocean Eng. 311, 118997.

Jia, H., Wu, Z., 2026. The impact of Russia-Ukraine war on international maritime petroleum trade and tanker fleet productivity. J. Transp. Geogr. 131, 104543.

Li, K.X., Wang, H., Yang, Y., Li, M., 2024. Resilience in maritime logistics: Theoretical framework, research methodology, and indicator system. Ocean & Coastal Management 259.

Li, J., Yao, X., Zhong, Y., Wang, H., 2026. Volatility connectedness and its sources between crude oil and commodity sectors: evidence from China. J. Commod. Mark. 42, 100558.

Liu, Q., Yang, Y., Ng, A.K.Y., Jiang, C., 2023. An analysis on the resilience of the European port network. Transp. Res. A Policy Pract. 175, 103778.

Lu, B., Sun, Y., Wang, H., Wang, J.-J., Shuai liu, s. & cheng, t. c. e., 2024. Dynamic resilience analysis of the liner shipping network: from structure to cooperative mechanism. Transportation Research Part e: Logistics and Transportation Review 191, 103755.

Mohsendokht, M., Mokhtari-Moghadam, A., Li, H., Kontovas, C., Chang, C.-H., Qu, Z., Yang, Z., 2026. A Risk-based simulation approach to assessing seaport resilience against cyclone hazards. Transp. Res. Part D: Transp. Environ. 154, 105291.

NIU, X., CHEN, W. & WANG, N. 2023. Spatiotemporal Dynamics and Topological Evolution of the Global Crude Oil Trade Network. *Energies* 2023; 16(4):1728.

Poo, M.C., Yang, Z., 2024. Optimising the resilience of shipping networks to climate vulnerability. Marit. Policy Manag. 51, 15–34.

Qin, Y., Guo, J., Wu, S., 2025. The resilience evolution and dynamic process identification of the global shipping network. Transp. Policy 174, 103851.

Sajedianfard, N., Shahnazi, R., 2025. Optimizing the crude oil trade network: Balancing cost and environmental impact. Energ. Strat. Rev. 62, 101900.
Seif, M., Tosarkani, B.M., Zolfagharinia, H., 2026. Enhancing humanitarian logistics under uncertainty: a data-driven distributionally robust optimization approach with worst-case mean-CVaR. Transportation Research Part e: Logistics and Transportation Review 205, 104516.
Shahnazi, R., Sajedianfard, N., Melatos, M., 2023. Import and export resilience of the global oil trade network. Energy Rep. 10, 2017–2035.
Shu, Y., Xiong, C., Zhu, Y., Liu, K., Liu, R.W., Xu, F., Gan, L., Zhang, L., 2024. Reference path for ships in ports and waterways based on optimal control. Ocean & Coastal Management 253, 107168.
Si, R., Jia, P., Li, H., Zhao, X., 2025. Assessing the structural resilience of the global crude oil maritime transportation network: a motif-based approach from network to ports. J. Transp. Geogr. 123, 104123.
Si, R., Wang, N., Jia, P., Li, H., Yuan, S., 2026. Unraveling structural shifts and resilience patterns of global and intercontinental crude oil maritime transportation networks under geopolitical conflicts: a multiplex network model. Transportation Research Part e: Logistics and Transportation Review 206, 104550.
Su, W., Zhang, L., Lu, J., Zhu, J., 2025. Crude oil maritime transportation network resilience assessment based on optimal strategies. Transport and Environment, Transportation Research Part D.
Su, W., Lu, J., Zhang, L., 2026. Enhancing the resilience of the global crude oil maritime transportation network: a multi-strategy perspective. Marit. Policy Manag. 1–31.
Tran, N.K., Haralambides, H., Notteboom, T., Cullinane, K., 2024. The costs of maritime supply chain disruptions: the case of the Suez Canal blockage by the 'ever given' megaship. Int. J. Prod. Econ.
Verschuur, J., Koks, E.E., Hall, J.W., 2023. Systemic risks from climate-related disruptions at ports. Nat. Clim. Chang. 13, 804–806.
Verschuur, J., Lumma, J., Hall, J.W., 2025. Systemic impacts of disruptions at maritime chokepoints. Nat. Commun. 16, 10421.
Wan, C., Yang, Z., Zhang, D., Yan, X., Fan, S., 2018. Resilience in transportation systems: a systematic review and future directions. Transp. Rev. 38, 479–498.
Wang, W., Yang, K., Yang, L., Gao, Z., 2021. Two-stage distributionally robust programming based on worst-case mean-CVaR criterion and application to disaster relief management. Transportation Research Part e: Logistics and Transportation Review 149, 102332.
Wang, N., Yuen, K.F., Gao, X., Nie, Y., 2025. Resilience assessment of global container shipping network via port communities. Transp. Res. Part D: Transp. Environ. 141, 104649.
Wang, T., Xu, T.Z., Feng, H., Guo, Z., Poo, M.-C.-P., Tang, J., Ng, A.K.Y., 2026. Enhancing port resilience to typhoon disasters: a framework for recovery optimization and shipping network impact assessment. Transp. Policy 180, 104029.
Xiao, R., Xiao, T., Zhao, P., Zhang, M., Ma, T., Qiu, S., 2024. Structure and resilience changes of global liquefied natural gas shipping network during the Russia–Ukraine conflict. Ocean & Coastal Management 252, 107102.
Xin, X., Yang, Z., 2026. Resilience assessment: Insights from port community structures across the global container shipping network. Reliab. Eng. Syst. Saf. 265, 111489.
Xu, X., Zhu, Y., Xu, M., Deng, W., Zuo, Y., 2022. Vulnerability analysis of the global liner shipping network: from static structure to cascading failure dynamics. Ocean & Coastal Management 229, 106325.
Xu, K., Cui, Y., Liu, J., 2024a. Modeling the resilience of liner shipping network under cascading effects: considering distance constraints and transportation time. Comput. Ind. Eng. 197, 110559.
Xu, M., Zhu, Y., Liu, K., K. y. ng, a., 2024b. Assessing resilience of global liner shipping network to tropical cyclones. Transp. Res. Part D: Transp. Environ. 131, 104189.
Yang, D., Wu, L., Wang, S., Jia, H., Li, K.X., 2019. How big data enriches maritime research – a critical review of Automatic Identification System (AIS) data applications. Transp. Rev. 39, 755–773.
Yang, H., Liu, C., Cao, Y., Shu, Y., Gan, L., Liu, Z., Yang, Z., 2026. Dynamic resilience assessment of global shipping networks against cascading effects: an AIS data-driven complex network analysis. Sustainable Horiz. 18, 100184.
Zhang, J., Xin, X., Dubey, R., Nguyen, T.T., Shi, X., Li, N., Yang, Z., 2025a. Impact of the Ripple effect on the Resilience of Multimodal Container Port Operations: a System Dynamics simulation Approach. Risk Anal. 45, 4903–4932.
Zhang, J., Xin, X., Liao, Z., Dubey, R., Nguyen, T.T., Li, N., Yang, Z., 2025b. Analysis of the ripple effects of disruptions on multimodal container terminals operations: a System Dynamics approach. Transportation Research Part e: Logistics and Transportation Review 202, 104264.
Zhang, H., Zhao, X., Wang, J., Huang, R., 2026a. Dynamic port resilience assessment in the maritime network: modeling flow evolution and cascading failure. Reliab. Eng. Syst. Saf. 267, 111927.
Zhang, L., Su, W., Liao, S., Wang, S., 2026b. Enhancing energy security through multi-scale network analysis: robustness in global crude oil shipping–trade networks. Reliab. Eng. Syst. Saf. 265, 111525.
Zhu, J., Lu, J., Su, W., 2025. Empirical analysis of global crude oil transportation network amid the Russia-Ukraine conflict. J. Transp. Geogr. 127, 104305.